



POLITECNICO DI TORINO

Department of Environment, Land and Infrastructure Engineering DIATI

Master of Science in Petroleum Engineering

Polymer Degradation in High pH Solutions and the Effect of Polymers on the Phase Behavior of Alkali-Oil

Supervisor:

Prof. Dario VIBERTI

Co-Supervisors:

Torsten CLEMENS, OMV GmbH

Rafael E. HINCAPIE R. OMV GmbH

Bettina SCHUMI, OMV GmbH

Candidate:

Jose Rene Felipe SARQUEZ BERNAL

APRIL 2019

ACKNOWLEDGEMENTS

I would like to express my gratitude to my supervisor, Dr. Dario Viberti, for his guidance and support since I started this Master Program.

I also express my deepest gratitude to Dr. Torsten Clemens, Bettina Schumi and Dr.-ing. Rafael Hincapie for giving me the opportunity to write my thesis at OMV, for their guidance, support and for their invaluable insights I needed to make this work a fulfilling experience. In addition, to Christian Einzinger, Thomas Gumpenberger and Munir for their contribution to this project.

I would like to express my deepest gratitude to my parents, my siblings and to Maria Fernanda for their endless love and support.

ABSTRACT

With a continuous increase in the worldwide demand for the crude oil and considering the fact that conventional oil and gas resources are depleting, the Enhanced Oil Recovery processes (EOR) play a vital role to boost the production from mature reservoirs. Chemical Enhanced Oil Recovery (cEOR) is one of the most implemented methods to produce the remaining oil in-situ. Alkali-Polymer flooding is a cEOR technique in which the alkali should react chemically with the oil to produce in-situ surfactants/soaps. Polymers solutions are expected to provide fluid mobility control and improve the sweep efficiency. Hence, it is crucial that the viscosity of a polymer solution does not decrease throughout its propagation along the reservoir.

The 16 Tortonian Horizon (TH) of the Matzen field has been screened for the application of different EOR and is considered a suitable candidate for Alkali-Polymer flooding due to its reactive oil properties (high acidity). This work presents a set of criteria/workflow for defining polymer degradation in high pH solutions using fluid samples from the 16 TH reservoir. Based on this workflow, the procedures and the effect of those solutions on the alkali-oil phases are described. This combination allows performing long-term polymer degradation screening in a partially degassed environment without using a glovebox. Long-term thermal stability was assessed for three commercial partially hydrolyzed polyacrylamide (HPAM).

The workflow can be divided into four different steps. First, an assessment of polymer viscosifying power behaviour -with different polymer concentrations- at reservoir temperature. Second, the definition of optimum polymer concentrations in presence of alkali (7500 ppm) for each of the three studied polymers. This approach aimed to reach viscosity values reported in previous micromodel/core flooding experiments. Third, Long-term stability assessment, including periodic steady-shear rheological, pH and dissolved oxygen measurements, to define effects of temperature (50-70°C), dissolved-oxygen and presence of alkali on viscosity and average molecular weight (MW). Finally, Phase-behaviour experiments with and without the presence of polymer, in order to define the effect of polymers in the phase behavior of alkali-oil mixtures.

The overall findings and observations presented in this work showed that the presence of alkali enhances the residual viscosity values for polymer solutions roughly 20% after 20 days. Moreover, the apparatus used for the degassed set can be used as an economic alternative to perform long-term stability assessments. Flopaam 3630 S and Flopaam 5205 VHM showed residual viscosities values ranged between 82% to 99% and 90% to 91% respectively for the

degassed set. In addition, solutions aged at 50°C showed a half-life time 4- to 10- times bigger in comparison with solutions aged at 60- and 70°C. For the phase experiments, polymer presence affects the phase behavior of alkali-oil solutions. It reduces the amount of water that can partition into the emulsion phase. Finally, no major differences in phase behavior were observed for the three studied polymers regardless of the temperature.

NOMENCLATURE

<u>Symbol</u>	<u>Definition</u>
$^{\circ}API$	API Gravity
$^{\circ}C$	Celsius Degree
FR	Filtration Ratio
Hz	Hertz
K	Permeability
m	Meters
M	Mobility Ratio
mD	Millidarcy
ml	Milliliters
mPa	Millipascal
MW	Molecular Weight
η_o	Oil Viscosity
η_w	Water Viscosity
\emptyset	Porosity
P	Pressure
s	Seconds
t	Time
v_o	Volume of Oil
v_w	Volume of Water

ABBREVIATIONS

<i>Symbol</i>	<i>Definition</i>
<i>AP</i>	Alkali, Polymer
<i>ASP</i>	Alkali, Surfactant, Polymer
<i>cEOR</i>	Chemical Enhanced Oil Recovery
<i>D. O</i>	Dissolved Oxygen
<i>EACN</i>	Equivalent Alkane Carbon Number
<i>EOR</i>	Enhanced Oil Recovery
<i>HPAM</i>	Partially Hydrolyzed Polyacrylamide
<i>IFT</i>	Interfacial Tension
<i>MW</i>	Molecular Weight
<i>PAM</i>	Unhydrolyzed Polyacrylamide
<i>ppb</i>	Parts Per Billion
<i>ppm</i>	Parts Per Million
<i>rpm</i>	Revolutions Per Minute
<i>ST</i>	Surface Tension
<i>TH</i>	Tortonian Horizon

CONTENTS

ACKNOWLEDGEMENTS	ii
ABSTRACT	iii
NOMENCLATURE	v
ABBREVIATIONS	vi
LIST OF FIGURES	x
1. INTRODUCTION	1
2. STATE OF THE ART AND FUNDAMENTS	3
2.1. Chemical Enhanced Oil Recovery (cEOR).....	4
2.2. Alkaline-Polymer Flooding	4
2.2.1. Alkali Effect	5
2.2.2. Polymer Effect	5
2.3. Alkali-Polymer Interactions	7
2.3.1. Alkali Effect in Polymer viscosity	7
2.3.2. Polymer Effect in IFT	8
2.4. Polymer Degradation	8
2.4.1. Biological Degradation	8
2.4.2. Chemical Degradation.....	8
2.4.3. Mechanical Degradation	10
2.5. Alkali-Oil Phase Behavior	11
2.5.1. Microemulsion Types.....	11
2.5.2. Microemulsion Screening	12
2.5.3. Microemulsion Viscosity	13
3. FIELD BACKGROUND, EQUIPMENT, EXPERIMENTAL APPROACH AND METHODOLOGY	14
3.1. Reservoir Background	14
3.2. Equipment.....	14

3.3.	Setup and Procedure	20
3.3.1.	Brine Softening	20
3.3.2.	Polymer Solution Preparation	21
3.3.3.	Preliminary Rheological Assessment Description	22
3.3.4.	Aging Experiments Description	22
3.3.5.	Phase Experiments Description.....	24
4.	EXPERIMENTAL RESULTS	27
4.1.	Polymer Viscosifying Power	27
4.2.	Polymer – AP Solutions Comparison	29
4.3.	Long-term Stability Assessment	30
4.3.1.	Baseline Set	30
4.3.2.	Degassed Set	32
4.3.3.	Temperature Set	34
4.4.	Phase Experiments	36
4.4.1.	Emulsions Stability in Time	36
4.4.2.	Phase Maps.....	39
5.	RESULTS ANALYSIS	43
5.1.	Polymer Viscosifying Power	43
5.2.	Polymer – AP Solutions Comparison	43
5.3.	Long-term Stability Assessment	43
5.3.1.	Baseline Set	43
5.3.2.	Degassed Set	44
5.3.3.	Temperature Set	45
5.4.	Phase Experiments	46
5.4.1.	Emulsions Stability in Time	46
5.4.2.	Phase Maps.....	47
6.	CONCLUSIONS	48

7. REFERENCES 49

LIST OF FIGURES

Figure 2-1. The Main Phases of a Field Development Plan, Modified from (Alvarado and Manrique, 2010). 3

Figure 2-2. EOR Methods Classification, Modified from (Gbadamosi et al., 2018). 4

Figure 2-3. Comparison of Residual Oil Recovery Factors in any Combination of Alkaline-Polymer Flood, Modified From (Krumrine and Falcone, 1987). 5

Figure 2-4. Sweep Efficiency Comparison between Waterflooding and Polymer Flooding. 6

Figure 2-5. Effect of Alkaline Concentration in Polymer Viscosity, Modified from (Kang, 2001). 7

Figure 2-6. Effect of Fe²⁺ Concentration in Polymer Viscosity, Modified from (Luo et al., 2006). 9

Figure 2-7. Relation between Degree of Hydrolysis and Viscosity, Modified from (Levitt et al., 2011). 10

Figure 2-8. (Winsor, 1954) Microemulsion Classification. 12

Figure 2-9. Typical Microemulsion Shifting when Increasing Salinity, (Sheng, 2015). ... 13

Figure 3-1. Dowex® Marathon™ C Sodium Form. 16

Figure 3-2. 16 TH Dead Oil Steady-Shear Rheology. 16

Figure 3-3. VWR pHenomenal® OX 4100 dissolved oxygen and pH meter. 17

Figure 3-4. Physica MCR 301 Rheometer. 18

Figure 3-5. Double-Gap Measuring System Geometry. 18

Figure 3-6. Rotating Shaker. 19

Figure 3-7. Brine Softening Process Description. 20

Figure 3-8. Polymer Solution Process Description. 21

Figure 3-9. Preliminary Rheological Assessment Process Description. 22

Figure 3-10. Aging Experiments Process Description. 23

Figure 3-11. Experimental Setup Utilized for Polymer Degassing 24

Figure 3-12. Phase Experiments Process Description 25

Figure 3-13. Dead Oil and Surrogated Oil Rheological Measurements 25

Figure 4-1. Polymers Rheological Behaviour at Different Concentrations 28

Figure 4-2. Polymers Viscosity Comparisson for Different Concentrations at a Shear Rate of 7.94s⁻¹ 28

Figure 4-3. Alkali-Polymers Rheological Behaviour at Different Concentrations 29

Figure 4-4. Alkali-polymers Viscosity Comparisson for Different Concentrations at a Shear Rate of $7.94s^{-1}$ 30

Figure 4-5. Baseline Set Viscosity over Time Comparisson at a Shear Rate of $7.94s^{-1}$ 31

Figure 4-6. Degassed Set Viscosity over Time Comparisson at a Shear Rate of $7.94s^{-1}$... 33

Figure 4-7. Residual Viscosity Comparison between External Experiments and Results from this Work 34

Figure 4-8. Temperature Set Viscosity over Time Comparisson at a Shear Rate of $7.94s^{-1}$ 35

Figure 4-9. Emulsion Volumes Phases Clarification..... 36

Figure 4-10. Phase Experiments Emulsion Volumes over Time at $50^{\circ}C$ 37

Figure 4-11. Phase Experiments Emulsion Volumes over Time at $60^{\circ}C$ 38

Figure 4-12. Phase Experiments Emulsion Volumes over Time at $70^{\circ}C$ 39

Figure 4-13. Phase Maps Nomenclature Clariffication 40

Figure 4-14. Phase Maps at $50^{\circ}C$ 40

Figure 4-15. Phase Maps at $60^{\circ}C$ 41

Figure 4-16. Phase Maps at $70^{\circ}C$ 42

LIST OF TABLES

Table 1-1: 16 TH Reservoir Properties and Sheng Screening Comparison 1

Table 3-1: 16 TH Properties. 14

Table 3-2: Auersthal Brine Composition..... 15

Table 3-3: Chemical Characteristics of the Evaluated Polymers. 15

Table 3-4: Chemical Characteristics of Na₂CO₃ Provided by Sigma Aldrich..... 17

Table 3-5: MCR 301 Rheometer Specifications..... 19

Table 3-6: Softened Auersthal Brine Composition..... 21

Table 3-7: Set of Experiments Defined for the Aging Evaluations 23

Table 3-8: Phase Experiments Description..... 26

Table 4-1. Polymer Defined Concentrations for Aging and Phase Experiments 30

Table 4-2. Baseline Dissolved Oxygen Concentration over Time 31

Table 4-3. Baseline Solutions pH over Time..... 31

Table 4-4. Degassed Solutions pH over Time 32

Table 4-5. Temperature Dissolved Oxygen Concentration over Time..... 35

Table 4-6. Temperature Solutions pH over Time 35

Table 5-1. Baseline Residual Viscosities Comparison 44

Table 5-2: Long-Term Temperature Set Results 46

1. INTRODUCTION

The 16 Tortonian Horizon (TH) of the Matzen field -located 20 km northeast of Vienna- is one of the largest reservoirs in Austria (Gruenwalder et al., 2007). Recently it has been screened for the application of different EOR methods as reported by (Lüftenegger and Clemens, 2017) and (Poellitzer et al., 2008). The 16 TH is considered a suitable candidate for Alkali-Polymer, due to its reactive oil properties (high acidity). Table 3-1 describes some of the most relevant properties of this reservoir and compares the values with the Alkali-Polymer screening proposed by (Sheng, 2017). Further reservoir characterization details are given by (Kienberger and Fuchs, 2006). Whereas, alkali should react chemically with the oil to produce in-situ surfactants. Polymers solutions are expected to provide fluid mobility control and improve the sweep efficiency. Hence, as stated by (Lake, 1989), (Pye, 1964), (Sheng, 2011a) and (Sorbie, 1991), it is crucial that the viscosity of a polymer solution does not decrease throughout its propagation along the reservoir.

Table 1-1: 16 TH Reservoir Properties and Sheng Screening Comparison

Property	16 th TH	Sheng Screening
Oil Viscosity [mPa.s]	~ 4-6	<150
Oil Gravity [°API]	25	NC
Temperature [°C]	60	<93.3
Mean Permeability [mDa]	1200	>50
TAN	2	Organic Acid
Formation Water Salinity [TDS, ppm]	~ 20,000	<50,000
Divalent [ppm]	~ 26*	<100

*Divalent concentration obtained after brine softening.

When applying Alkali-Polymer flooding, the process becomes more complex since polymers will not only interact with the rock matrix and reservoir fluids but also with the alkali agent (Kazemi Nia Korrani et al., 2016). According to the literature, there are two main ways in which alkali can affect polymer viscosity. First, alkali contributes to the hydrolyzation of the polymer over time and therefore it helps to increase polymer viscosity. Second, alkali will decrease the initial polymer viscosity due to an increase in water salinity. Overall, as stated by (Levitt et al., 2011), (Sheng et al., 1994) and (Yang et al., 2010), polymer solution viscosity may either decrease or increase by coupling both mechanisms. Moreover, caustic/alkaline flooding is known by the emulsification of crude oil by soap into the high pH water phase forming an oil-in-water (O/W) emulsion. These emulsions may display high viscosities and

therefore influence the final oil recovery (Fortenberry et al., 2015), (Nelson et al., 1984), (Sheng, 2011c) and (Sheng, 2017).

Research in recent years has focused on the effect of the temperature and oxygen content in polymer solution degradation, especially in the presence of divalent cations such as iron calcium or magnesium (Levitt et al., 2011), (Moradi-Araghi and Doe, 1987), (Ryles, 1988) and (Seright and Skjevraak, 2015). A common way to assess the degradation is by using rheological assessments and phase behavior experiments. Consequently, oxygen content and temperature effects are two major concerns and therefore are considered in this work.

This work presents a set of criteria/workflow for defining polymer degradation in high pH solutions. Based on this workflow, the procedures and the effect of those solutions on the alkali-oil phases are described. This combination allows performing long-term polymer degradation screening in a partially degassed environment without using a glovebox. Long-term thermal stability was assessed for three commercial partially hydrolyzed polyacrylamide (HPAM) using real injection softened water. The work can be divided in four different steps:

1. An assessment of polymer viscosifying power behaviour -with different polymer concentrations- at reservoir temperature.
2. Definition of optimum polymer concentrations in presence of alkali (7500 ppm) for each of the three studied polymers. This approach aimed to reach viscosity values reported in previous micromodel/core flooding experiments.
3. Long-term stability assessment, including periodic steady-shear rheological, pH and dissolved oxygen measurements, to define effects of temperature (50-70°C), dissolved-oxygen and presence of alkali on viscosity and average molecular weight (MW).
4. Phase-behaviour experiments with and without presence of polymer in order to define the effect of polymers in the phase behavior of alkali-oil mixtures.

2. STATE OF THE ART AND FUNDAMENTALS

With conventional oil fields depleting and the increase in the global energy demand, Enhanced Oil Recovery (EOR) has become more and more relevant in the oil and gas industry (Abidin et al., 2012), (Alvarado and Manrique, 2010) and (Sheng, 2011a).

EOR is generally defined as the last productive stage for a hydrocarbon reservoir, Figure 2-1. The Society of Petroleum Engineers defined EOR as “the technique or process where the physicochemical properties of the rock are changed to enhance the recovery of hydrocarbon. The properties of the reservoir fluid system which are affected by EOR process are chemical, biochemical, density, miscibility, interfacial tension (IFT)/surface tension (ST), viscosity and thermal”.

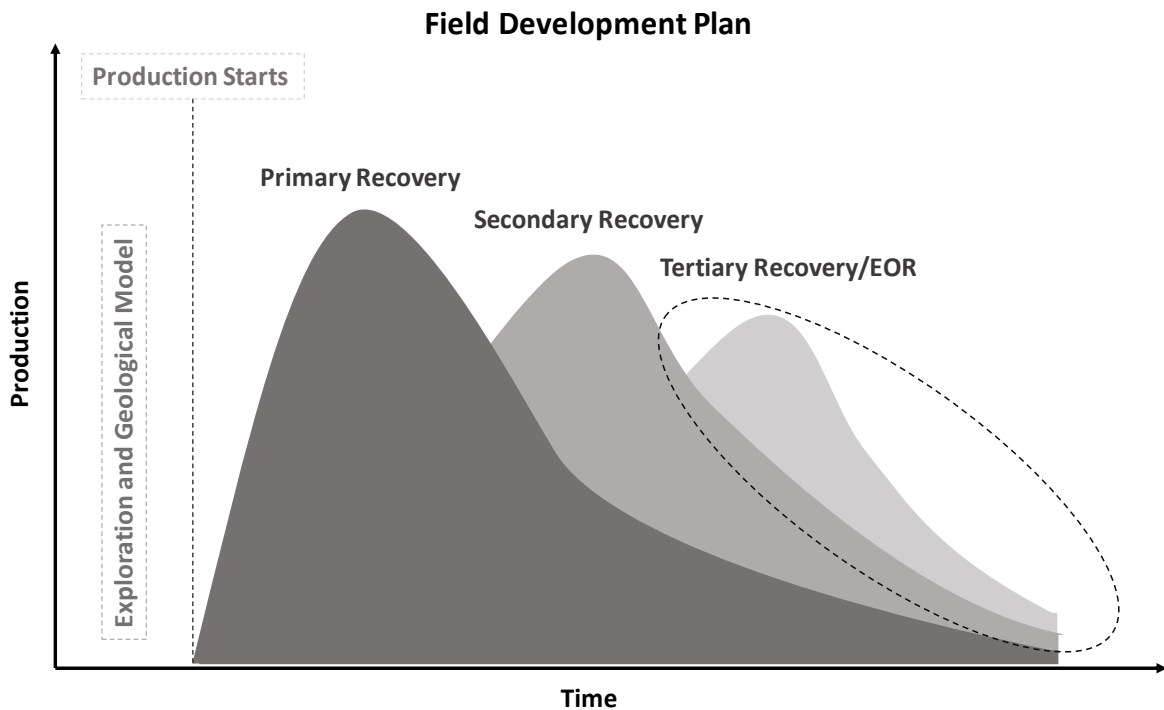


Figure 2-1. The Main Phases of a Field Development Plan, Modified from (Alvarado and Manrique, 2010).

At the same time, EOR can be divided into four different groups, Figure 2-2, This work will focus on Alkaline-Polymer, a type of Chemical Enhanced Oil Recovery (cEOR).

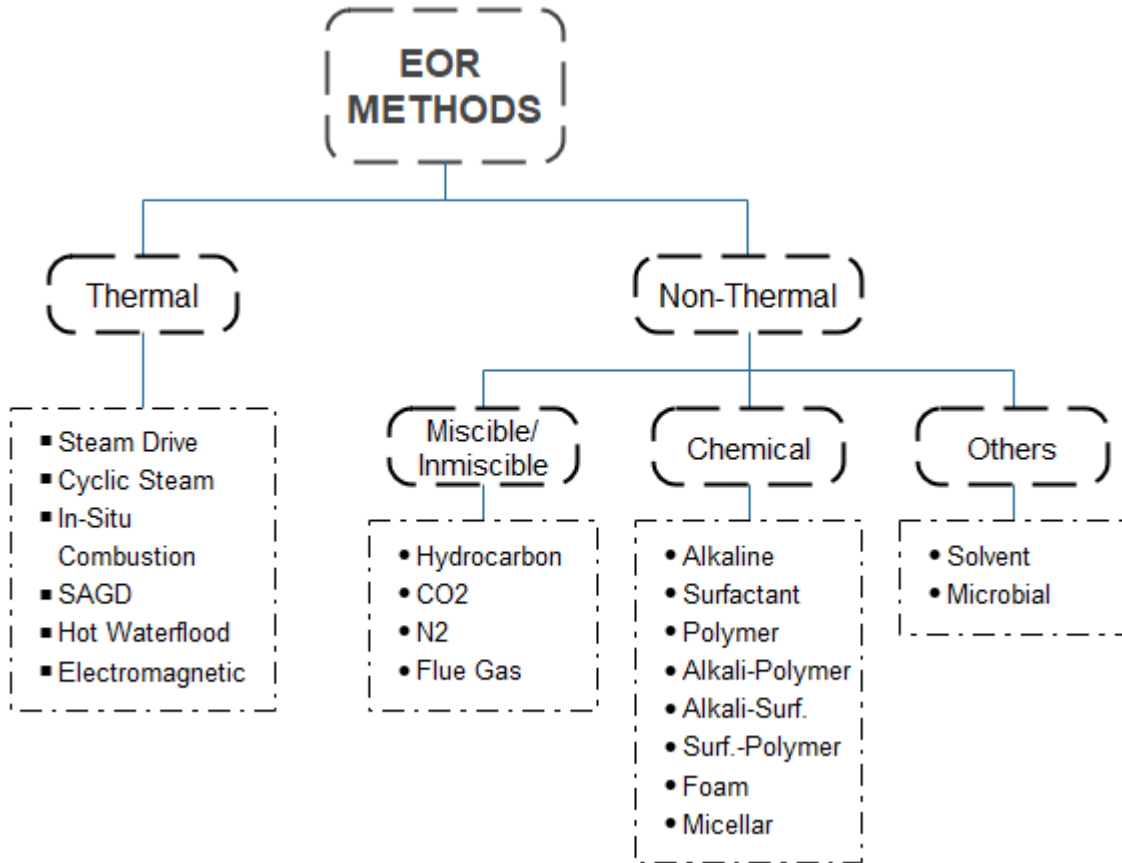


Figure 2-2. EOR Methods Classification, Modified from (Gbadamosi et al., 2018).

2.1. Chemical Enhanced Oil Recovery (cEOR)

cEOR refers to the process of injecting chemical compounds into the reservoir in order to enhance improve the oil displacement. Even though the cEOR can involve the injection of micellar, emulsion and foam components, the most used ones are Polymer (P), Alkaline (A) and Surfactants (S) or any combination of them (Johnson, 1976), (Sheng, 2011c) and (Yang et al., 2010).

2.2. Alkaline-Polymer Flooding

Alkali-Polymer flooding refers to any combination of Alkaline and Polymer flooding: (1) Alkaline followed by Polymer, (2) Polymer followed by Alkaline, or, (3) Alkaline and Polymer injected at the same time. Research performed by (Chen et al., 1999), (Krumrine and Falcone, 1987) and (Sheng, 2011c) regarding the synergy of the two components have reached the conclusion that, as shown in Figure 2-3, the higher incremental oil recovery is obtained when the two are injected simultaneously. The alkaline and polymer effects and drive mechanisms will be addressed later in this work.

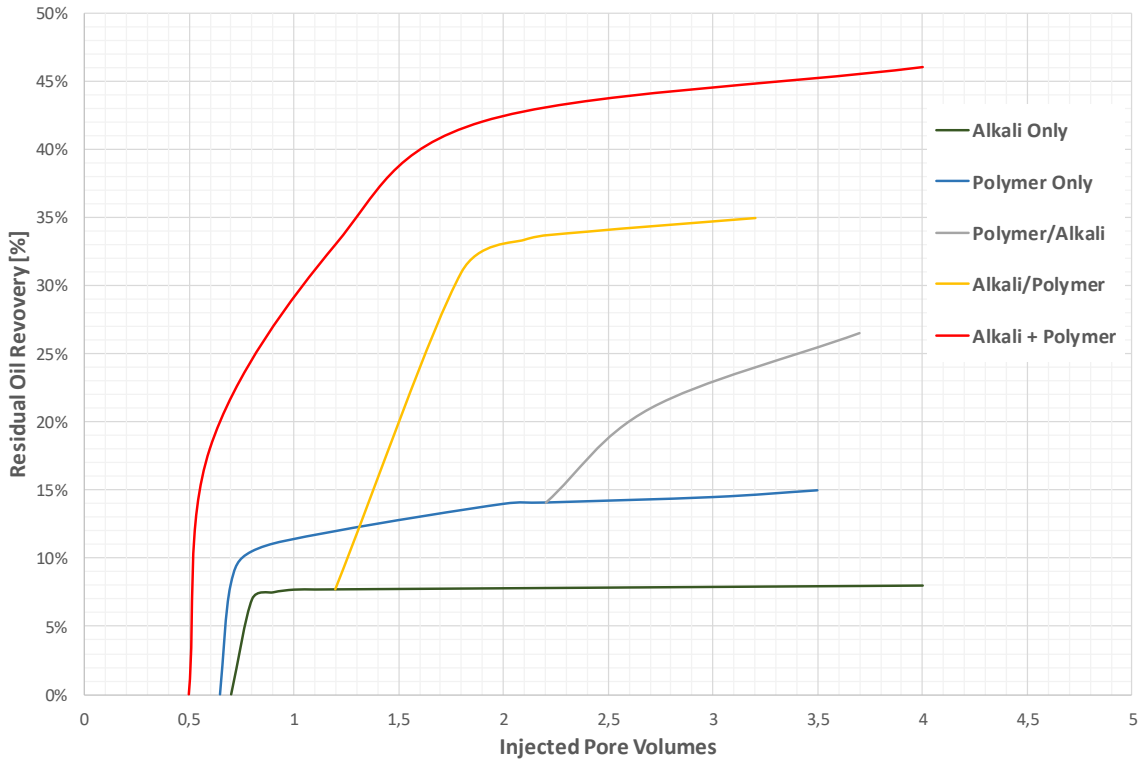


Figure 2-3. Comparison of Residual Oil Recovery Factors in any Combination of Alkaline-Polymer Flood, Modified From (Krumrine and Falcone, 1987).

2.2.1. Alkali Effect

There are five (5) proposed mechanisms in which alkaline enhances the oil recovery. (1) Emulsification of crude oil by soap into the flowing, high pH water phase, forming an oil-in-water (O/W) emulsion; (2) wettability reversal from oil-wet to water-wet, lowering relative permeability to the water and improving sweep efficiency; (3) wettability reversal from water-wet to oil-wet, reducing residual oil saturation; (4) emulsification and entrapment of viscous emulsions, diverting flow by blocking smaller pore throats; and (5) emulsification and coalescence, in which oil-in-water emulsions break spontaneously, locally increasing oil saturation and relative permeability to the oil. It is important to point out that as explained by (Fortenberry et al., 2015) and (Sheng, 2011b), IFT reduction is not mentioned as one of the drive mechanisms even though this emulsification and wettability reversal involve lowered IFT. The lowering of IFT was first introduced by (Nelson et al., 1984) when he published his work of what today is known as ASP flooding.

2.2.2. Polymer Effect

Polymers are macromolecules with a molecular weight in the order or millions of grams per mole. They provide mobility control during chemical flooding by increasing the viscosity of

the injected fluid. Good mobility control is achieved when the mobility ratio (M), is low (Chon and Yu, 2001) and (Sorbie, 1991).

$$M = \frac{k_{rw} * \eta_o}{k_{ro} * \eta_w} \quad (2.1)$$

Where k_{rg} is relative permeability to the gas, k_{ro} relative permeability to the oil, η_o oil viscosity and η_w water viscosity.

As stated by (Davis et al., 1968) and (Gogarty and Tosch, 1968), if M is smaller than the unity, fingering is avoided, Figure 2-4, this means that both areal and vertical sweep efficiencies are improved.

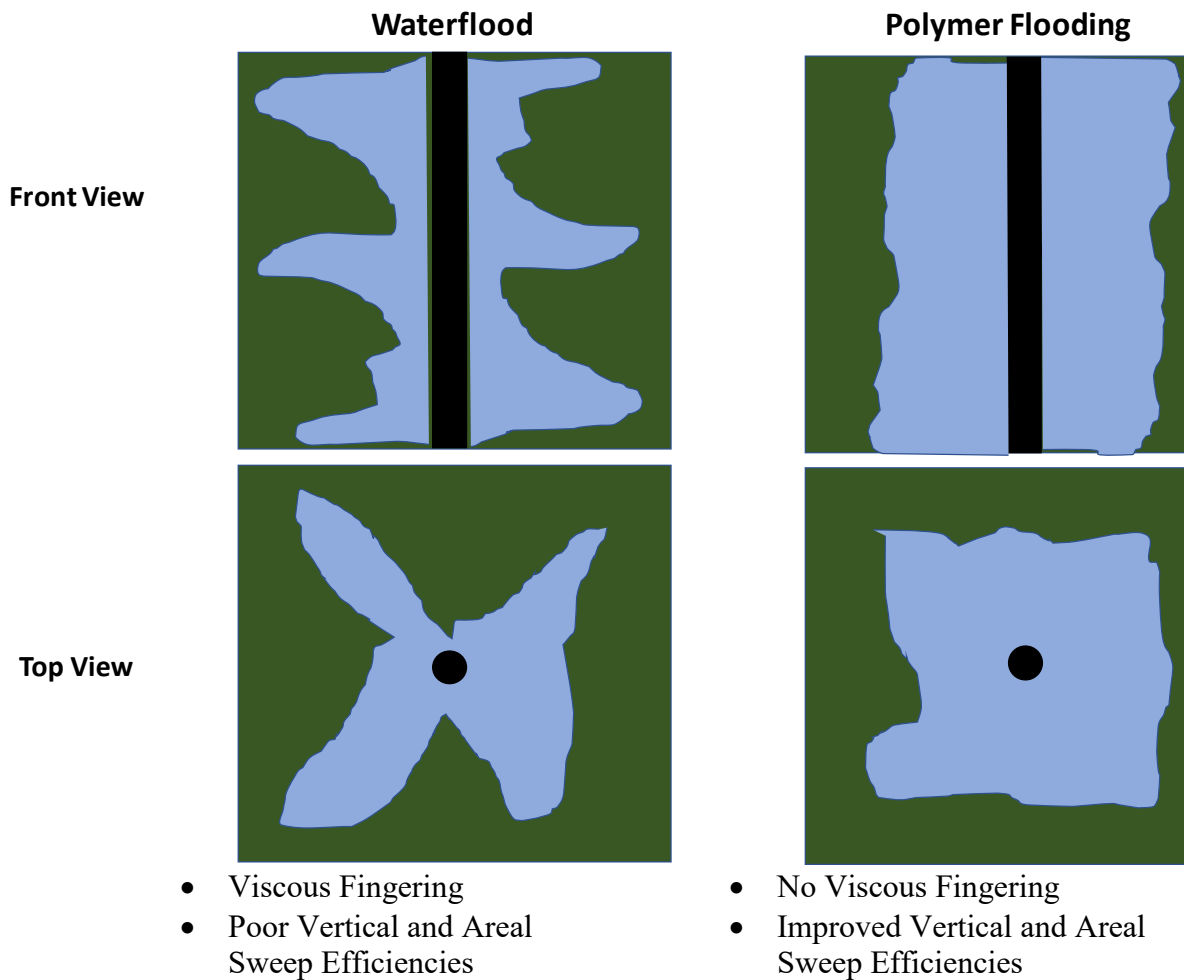


Figure 2-4. Sweep Efficiency Comparison between Waterflooding and Polymer Flooding.

There are different types of polymers, the most common ones are synthetic such as Unhydrolyzed Polyacrylamides (PAM) and Partially Hydrolyzed Polyacrylamide (HPAM) or biopolymers such as xanthan gum (Gaillard et al., 2015), (Needham and Doe, 1987) and (Sheng,

2011a). The most used for polymer flooding as well as all polymers using for this work is the HPAM. HPAM are polymers with molecular weight that variate from 1 to more than 20 million grams per mol (Gregory, 1984). Polymer selection is an arduous process since the behavior of the polymer is affected by many variables (Gaillard et al., 2015), (Guo, 2017), (Levitt and Pope, 2008) and (Sheng, 2017). Thus, a deep polymer study is required before the implementation of it on a field scale.

2.3. Alkali-Polymer Interactions

Alkali-Polymer interactions can be defined as the series of effects that occur when both substances are injected together and that do not occur when these substances are injected alone.

2.3.1. Alkali Effect in Polymer viscosity

Several authors have studied the effect of alkali in polymer viscosity (Alam and Tiab, 1985), (Levitt et al., 2011), (Sheng et al., 1994) and (Yang et al., 2010). There are two main ways in which alkali can affect polymer viscosity. First, alkali contributes to the hydrolyzation of the polymer over time and therefore it helps to increase polymer viscosity. Second, alkali will decrease initial polymer viscosity due to the increase in water salinity, Figure 2-5. In the end, viscosity may either decrease or increase by coupling both mechanisms.

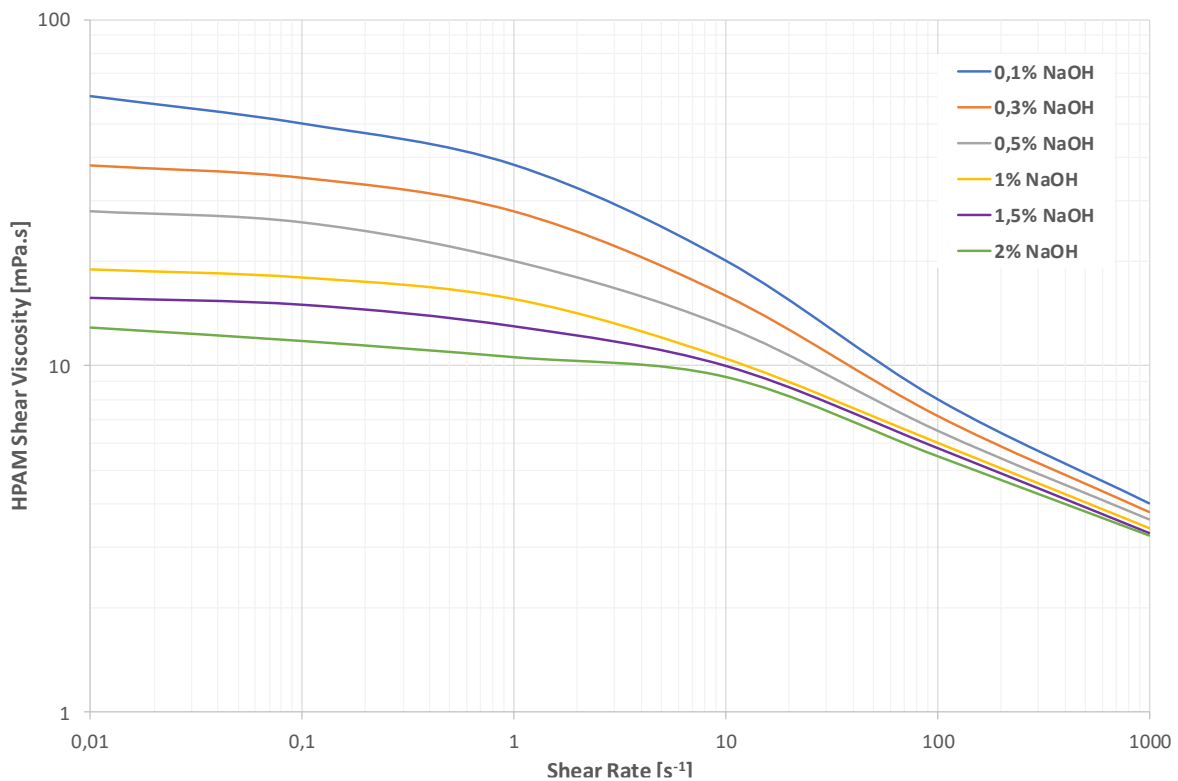


Figure 2-5. Effect of Alkaline Concentration in Polymer Viscosity, Modified from (Kang, 2001).

2.3.2. Polymer Effect in IFT

Polymer effect in IFT is complex and there is no agreement in the effect on how the polymers affect the alkali-oil IFT. Several authors (De-Qiang et al., 1993), (Potts and Kuehne, 1988) and (Sheng et al., 1994) state that since polymers have a small amount of surfactant, they may decrease the IFT. Moreover, (Suniga et al., 2016) showed that equilibrium is reached faster when polymer existed in the solution.

2.4. Polymer Degradation

One of the most important variables in polymer selection is the correct assessing of polymer degradation. Degradation refers mainly to the breakdown of polymer molecules that lead to viscosity losses. There are three main types of polymer degradation: (1) Biological Degradation (2) Chemical Degradation, (3) Mechanical Degradation.

2.4.1. Biological Degradation

It is induced by bacteria that cause macromolecules breakdown and therefore a loss in viscosity (Wellington, 1983). This type of degradation is important only for biopolymers and can be avoided by using biocides such as formaldehyde. The main issues on it as a degradation preventer is the fact that it is toxic and that the use of it may alter the other chemicals used for polymer protection such as oxygen scavengers.

2.4.2. Chemical Degradation

Chemical degradation is generally the main cause of polymer degradation. It is very complex and involves different variables such as dissolved oxygen, dissolved ions, hydrolysis, and, temperature as stated by (Clifford and Sorbie, 1985), (Levitt et al., 2011), (Muller et al., 1980) and (Ryles, 1988).

Dissolved Oxygen Effect (DO)

Dissolved oxygen is one of the main causes of chemical degradation. Due to its high redox potential, oxygen will lead to oxidative degradation of the polymer. Several authors have studied the effect of DO in polymer stability (Jouenne et al., 2017), (Luo et al., 2006) and (Yang and Treiber, 1985). In general, it can be said that oxidative degradation is proportional to the temperature and that oxygen content should be kept as low as possible by means of oxygen scavengers or degassed processes along with gas blankets or methanol to protect the polymer.

Dissolved Ions Effect

The presence of ions, especially divalent cations, have a major impact in polymer viscosity. Among all divalent cations, Fe^{2+} is known as the most critical one for polymer viscosity (Jouenne et al., 2017) and (Seright and Skjevrak, 2015). Experiments run by (Luo et al., 2006), shown in Figure 2-6, show that if dissolved oxygen is not removed, viscosity may drop by nearly 100% in 3 hours when Fe^{2+} is present in the solution,. Similar results were obtained by (Seright and Skjevrak, 2015) when oxygen concentration was around 5 ppm.

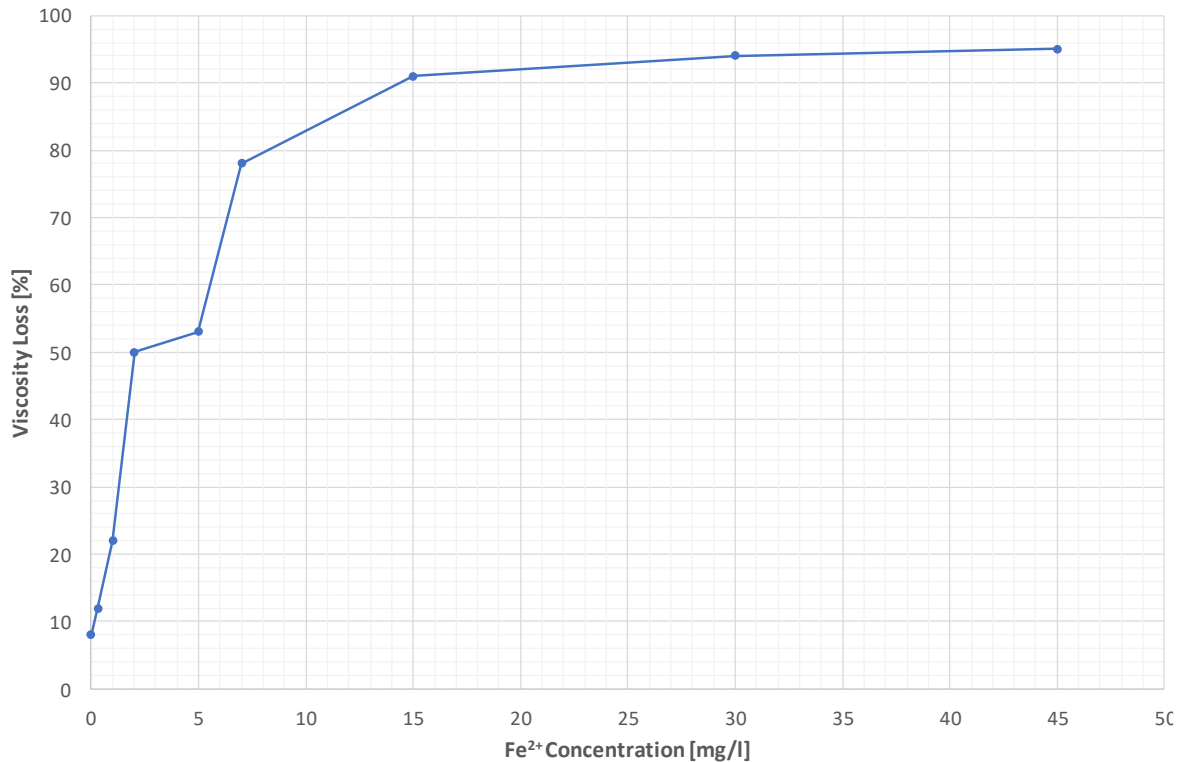


Figure 2-6. Effect of Fe^{2+} Concentration in Polymer Viscosity, Modified from (Luo et al., 2006).

The presence of calcium and Magnesium also affect polymer stability and have been studied by several authors (Davison and Mentzer, 1982), (Moradi-Araghi and Doe, 1987) and (Ryles, 1988). They noted that divalent cations not only reduce polymer viscosity but also, they lead to precipitation that may plug the pores.

Hydrolysis Effect

Hydrolysis is defined as the partition of molecules in presence of water. As stated by (Levitt et al., 2011), (Muller et al., 1980) and (Shupe, 1981) it is mainly affected by temperature. One parameter used to assess how stable is a polymer is the viscosity retention also called residual viscosity.

$$\text{Residual Viscosity} = \frac{\eta - \eta_{Brine}}{\eta_{initial} - \eta_{Brine}} \quad (2.2)$$

Where $\eta_{initial}$ is initial polymer viscosity, η is polymer viscosity at a given day and μ_{Brine} is brine viscosity.

(Kong, 1996) found that higher viscosity retention values were obtained at 40-50 % of hydrolysis. (Levitt et al., 2011) studied the chemical degradation under alkaline conditions and found that the degree of hydrolysis is dependent on pH and initial degree of hydrolysis. The values they reported for unhydrolyzed polyacrylamides, Figure 2-7, show that higher residual viscosities are aligned with the findings by (Kong, 1996).

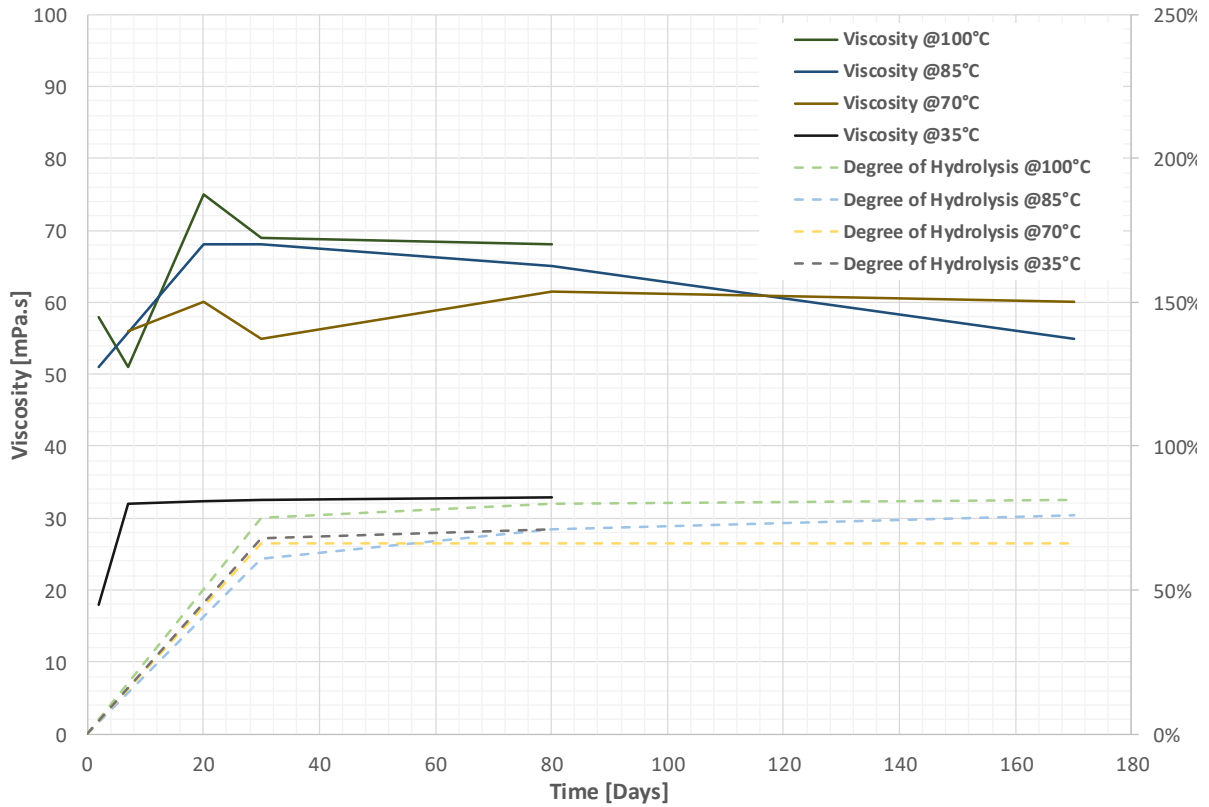


Figure 2-7. Relation between Degree of Hydrolysis and Viscosity, Modified from (Levitt et al., 2011).

2.4.3. Mechanical Degradation

Mechanical degradation occurs as a result of high mechanical stresses on the polymer macromolecules (Jouenne et al., 2015). This type of degradation is important near the wellbore and in polymer handling equipment (Sheng, 2011a). (Åsen et al., 2018) studied the degradation at cm and meter scales. (Puls et al., 2016) studied this mechanical degradation also during reservoir propagation and production. (Jouenne et al., 2018) investigated the polymer

mechanical stability after successive mechanical degradation events. In general, authors concluded that mechanical degradation depends on flow rate and geometry.

One parameter to characterize polymer stability is the filtration ratio (FR). It consists in pass the solution through a filter. In general, FR should be a value below 1.5 to be acceptable.

$$FR = \frac{t_{200} * t_{180}}{t_{100} * t_{80}} \quad (2.3)$$

Where t_{200} , t_{180} , t_{100} and t_{80} are the times in which 200, 180, 100 and 80 milliliters of solution have been filtered.

2.5. Alkali-Oil Phase Behavior

The understanding of alkali-oil phase behavior is crucial for the application of AP flooding. A third thermodynamic stable phase (microemulsion) can be formed in with oil and water-alkaline mixtures (Canter et al., 1982) and (Winsor, 1954). In AP flooding, the microemulsion is a distinct phase consisting of alkali, oil, and water. However, in other chemical flooding methods, it may include also co-solvents, co-surfactants and other components (Nelson et al., 1984) and (Rudin et al., 1994).

2.5.1. Microemulsion Types

Microemulsion classification was first done by (Winsor, 1954). He divided them in Type I (under-optimum conditions), Type II (over-optimum conditions), Type III (optimum conditions) and Type IV, Figure 2-8. Type I microemulsion, also known as Type II (-) is an oil-in-water microemulsion, where a portion of the oil has been solubilized into the surfactant micelles resulting in a two-phase Oil/Microemulsion system. A Type II microemulsion, also known as Type II (+), is a water-in-oil microemulsion, where a portion of the water has been solubilized in the surfactant micelles resulting in a two-phase Microemulsion/Water system. A Type III microemulsion is a three-phase system where both oil and water solubilized partially into the surfactant micelles. A Type IV microemulsion is a single-phase emulsion where both oil and water are completely solubilized into the surfactant micelles.

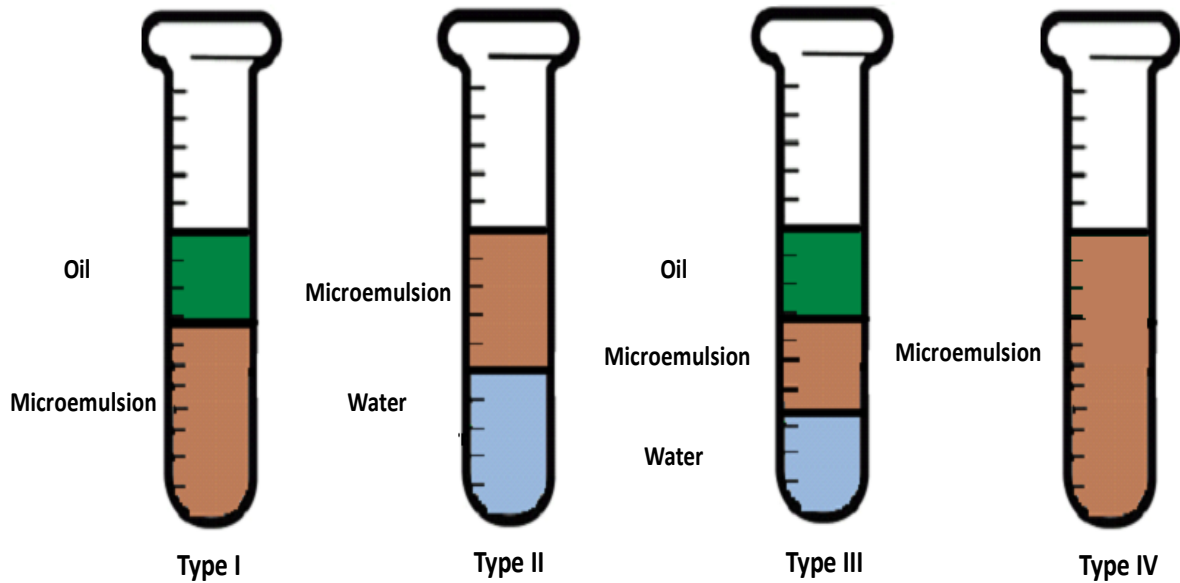


Figure 2-8. (Winsor, 1954) Microemulsion Classification.

2.5.2. Microemulsion Screening

Phase behavior is normally studied performing a phase screening. This is done by keeping fixed all variables except one. The most common analyzed variables are salinity, alkaline, surfactant and co-surfactant (Ajith and Animesh, 1994), (Gao et al., 1995), (Levitt et al., 2016), (Sheng, 2011d), (Unsal et al., 2015) and (Wegner and Ganzer, 2017). However, phase screening can be performed for other variables such as temperature, pressure and equivalent alkane carbon number (EACN) of the oil (Bourrel and Schechter, 1988), (Austad et al., 1998) and (Green and Willhite, 1998). An increase in hardness (addition of alkali) or salinity (addition of NaCl) will normally cause a Type I to Type III to Type II shift, Figure 2-9. However, since crude oil is a complex mixture of more than 200 organic compounds, phase-shift do not always present the same characteristic behavior when salinity/hardness increase. (Sagi et al., 2013) and (Wegner and Ganzer, 2017) reported a Type I to Type II transition without any observation of a Type III microemulsion but with the formation of a viscous macroemulsion for high salinity concentrations.

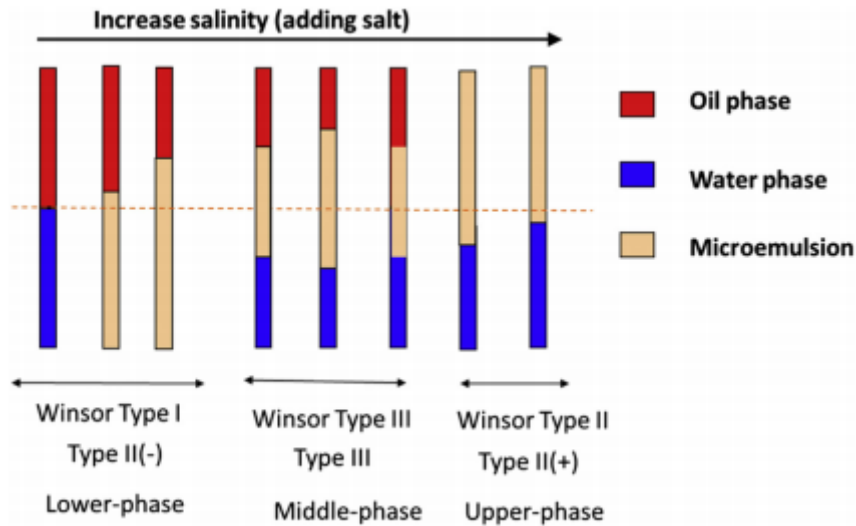


Figure 2-9. Typical Microemulsion Shifting when Increasing Salinity, (Sheng, 2015).

An increase in temperature typically generates a Type II to Type III to Type I for anionic surfactants although adding enough propylene oxide to the structure will generate the opposite behavior (Bourrel and Schechter, 1988), (Healy et al., 1976), (Salager et al., 1979) and (Skauge and Fotland, 1990).

2.5.3. Microemulsion Viscosity

Microemulsion viscosity is an important parameter in the design of an AP flooding. If the viscosity is too high, viscous fingering problems may appear. Also, it may depict an undesired non-Newtonian rheological behavior (Bennett et al., 1981) and (Suniga et al., 2016).

In Alkali/Oil or Surfactant/Oil mixtures, microemulsion viscosity behavior is well defined. In the case of Winsor Type I and Type II systems are very close to the viscosity of continuous oil and aqueous phases (Sagi et al., 2013) and (Suniga et al., 2016). For Winsor Type III, where there is a bicontinuous phase, larger viscosity values are observed as reported by (Suniga et al., 2016), (Tagavifar et al., 2018) and (Walker et al., 2012). On the other hand, when polymer is added to the mix, there is not a clear consensus on its effect in Type III microemulsion viscosities. (Tagavifar et al., 2018) stated that Polymer presence does not affect Type II and Type III viscosity values, which means that Polymer molecules do not partition into the macroemulsion phase. However, (Suniga et al., 2016) stated that the presence of polymer increased the viscosity of both Type I and Type III macroemulsions, which means that Polymer molecules can partition into the microemulsion phase.

3. FIELD BACKGROUND, EQUIPMENT, EXPERIMENTAL APPROACH AND METHODOLOGY

In this chapter, a backdrop for the results presented in Chapter 4 is set. The subsequent include a full description of all the experimental equipment used for the development of the thesis is presented. This includes brine softening process, polymer solution preparation, steady-shear rheological measurements, and phase experiments.

3.1. Reservoir Background

The 16 Tortonian Horizon (TH) of the Matzen field -located 20 km northeast of Vienna- is one of the largest reservoirs in Austria (Gruenwalder et al., 2007). Recently it has been screened for the application of different EOR methods as reported by (Lüftenegger and Clemens, 2017) and (Poellitzer et al., 2008). The 16 TH is considered a suitable candidate for Alkali-Polymer, due to its reactive oil properties (high acidity). Table 3-1 describes some of the most relevant properties of this reservoir. Further reservoir characterization details are given by (Kienberger and Fuchs, 2006).

Table 3-1: 16 TH Properties.

Property	Value
Oil Viscosity [mPa.s]	~ 4-6
Oil Gravity [°API]	25
Temperature [°C]	60
Mean Permeability [Da]	1.2
Min Permeability [mDa]	18
Max Permeability [Da]	10
Initial OWC [m]	1490
Initial GOC [m]	1455
TAN	2
Min Porosity [%]	17
Max Porosity [%]	40
Mean Porosity [%]	27
Oil Sand Net Thickness [m]	17

3.2. Equipment

This section describes all the materials that were necessary to perform all the experiments for the elaborations of this work. This includes reservoir fluids, chemicals, and laboratory equipment.

Reservoir Brine

Production brine from the 16 TH Reservoir, called Auersthal brine in this work, was collected from the outlet of the water treatment plant in Schönkirchen. Table 3-2 summarizes the 16 TH formation water composition and hardness properties.

Table 3-2: Auersthal Brine Composition.

Element	Auersthal Brine
	mg/l
Li ⁺	1.99
Na ⁺	7460.00
NH ₄ ⁺	55.60
K ⁺	75.80
Mg ²⁺	78.20
Ca ²⁺	145.00
Sr ²⁺	20.50
Ba ²⁺	14.40
Fe ^{2+,3+}	0.07
Total Hardness [dH°]	42.03

Polymers

Three polymers were studied in this work. Polymer selection was based on previous results obtained at OMV-TCL (Lüftenegger and Clemens, 2017) and (Clemens et al., 2013) and recommendations given by the vendor. The used polymers are chemically described in Table 3-3.

Table 3-3: Chemical Characteristics of the Evaluated Polymers.

	Flopaam 3630 S	Flopaam 5205 VHM	Flopaam 6030
Chemistry	Acrylamide/ Acrylate	Acrylamide/ATBS/ Acrylic acid polymer	Homopolymer Post- Hydrolyzed Acrylamide
Annicity	Medium to High	Medium	High
Molecular Weight	Medium	High	High

Ion-Exchange Resin

Dowex® Marathon™ C sodium form provided by Sigma Aldrich, see Figure 3-1 was used for water softening in order to avoid any problems of precipitation already described in section (2.4.2).



Figure 3-1. Dowex® Marathon™ C Sodium Form.

Dead Oil

Dead oil was collected from the 16 TH reservoir. It was degassed and dewatered before it was used in any experiment. Dead oil steady-shear rheology was measured and is displayed in Figure 3-2. Rheological data is also available in.

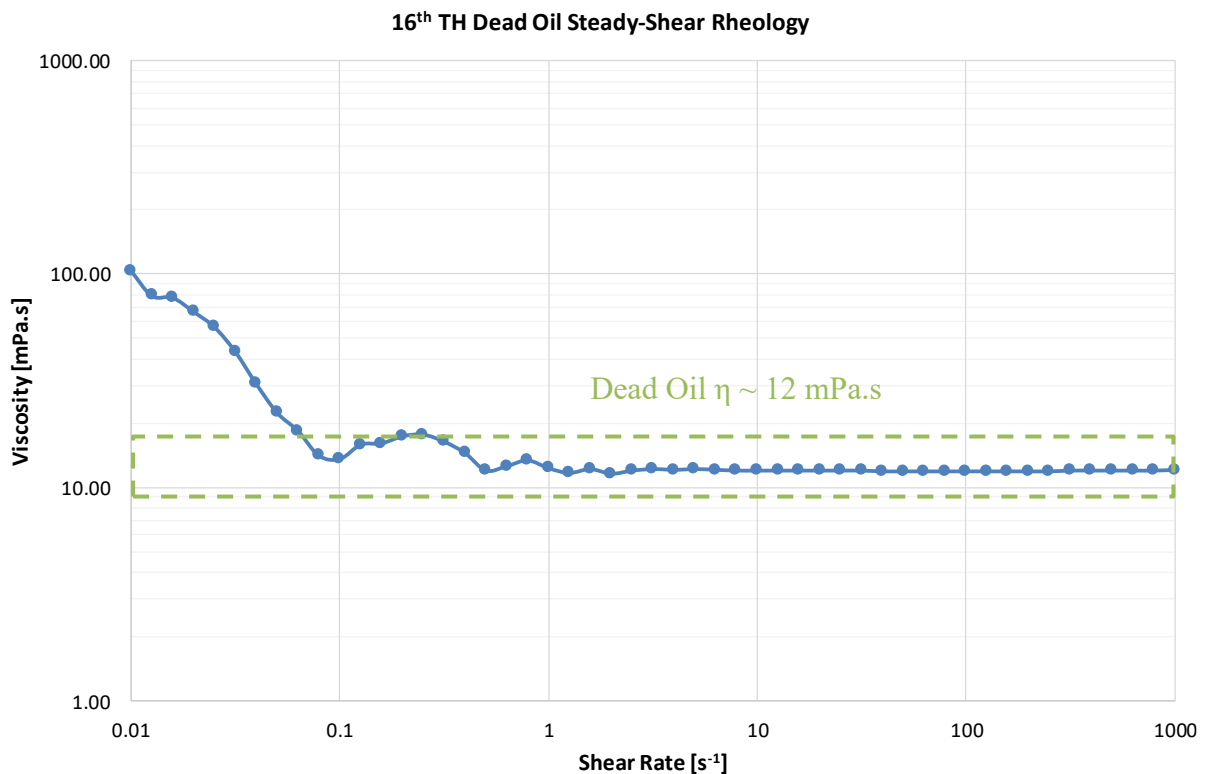


Figure 3-2. 16 TH Dead Oil Steady-Shear Rheology.

Alkaline Agent

Sodium carbonate (Na_2CO_3) was the alkaline agent used in all Alkali-Polymer solutions. It was provided by Sigma Aldrich and is described chemically in Table 3-4.

Table 3-4: Chemical Characteristics of Na₂CO₃ Provided by Sigma Aldrich.

Purity	≥99.0%
Form	powder
Impurities [%]	P: ≤0.02
	Insoluble matter: ≤0.1
Solubility at 20°C [g/l]	217
Anion Traces [%]	Cl: ≤0.05
	SO ₄ ²⁻ : ≤0.02
Cation Traces [%]	Al: ≤0.001
	Ca: ≤0.02
	Cu: ≤0.0005
	Fe: ≤0.001
	K: ≤0.005
	Mg: ≤0.005
	NH ₄ ⁺ : ≤0.05
	Pb: ≤0.001
Zn: ≤0.0005	

Convection Ovens

Convection ovens were used to maintain the temperature constant over time either at 50°C, 60°C or 70°C. They were used for aging and phase experiments.

pH and Dissolved Oxygen Meter

A pHenomenal® OX 4100 dissolved oxygen [D.O] and pH meter, see Figure 3-3 was used to keep track of this variable during experiments. Device resolution was 0.1 mg/l and 0.001 for D.O and pH respectively.



Figure 3-3. VWR pHenomenal® OX 4100 dissolved oxygen and pH meter.

Rheometer

A Physica MCR 301 Rheometer developed by Anton Paar with a double-gap measuring system, see Figure 3-4 and Figure 3-5, was used for the steady-shear rheological measurements performed for this work. Table 3-5 describes some of the specifications of this device.

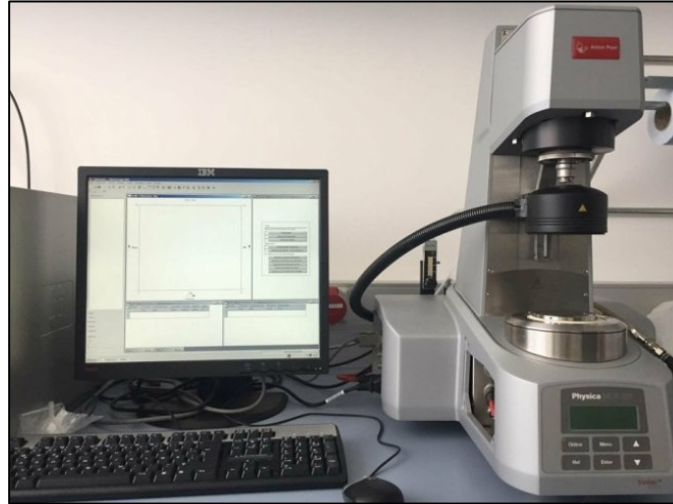


Figure 3-4. Physica MCR 301 Rheometer.

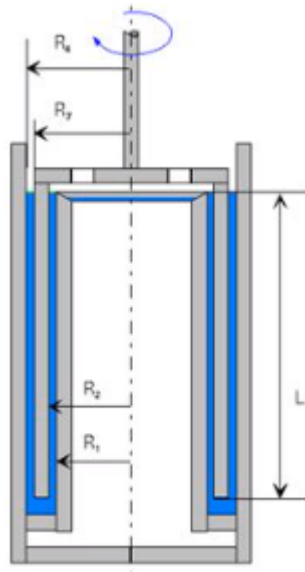


Figure 3-5. Double-Gap Measuring System Geometry.

Table 3-5: MCR 301 Rheometer Specifications.

Specification	
Frequency Range	10 ⁻⁵ – 10 ² Hz
Temperature Range	-40 – 200°C ± 0.01°C (Peltier-control)
Geometry	Coaxial double gap (DG26.7): gap width: 0.42 mm and 0.46 mm; sample volume: 3.8 ml; for low-viscosity samples (0.4 mPas < η < 200 mPas)
shear rate range	10 ⁻⁵ – 10 ⁴ s ⁻¹

Borosilicate Pipettes

All phase behaviour experiments were performed using 10 ml Fisher borosilicate pipettes with a graduation of 0.1 ml. This type of pipettes have been widely utilized in phase screening experiments (Fortenberry et al., 2015), (Puerto et al., 2015) and (Tagavifar et al., 2018).

Oxygenated Methane Torch

Borosilicate pipettes were sealed by means of an oxygenated methane torch. The mixture of methane and oxygen created a flame that reaches a temperature high enough to melt and fuse the pipette ends.

Rotating Shaker

A rotating shaker, shown in Figure 3-6, was used to ensure proper contact between the alkali-rich solutions and the oil during the phase experiments.

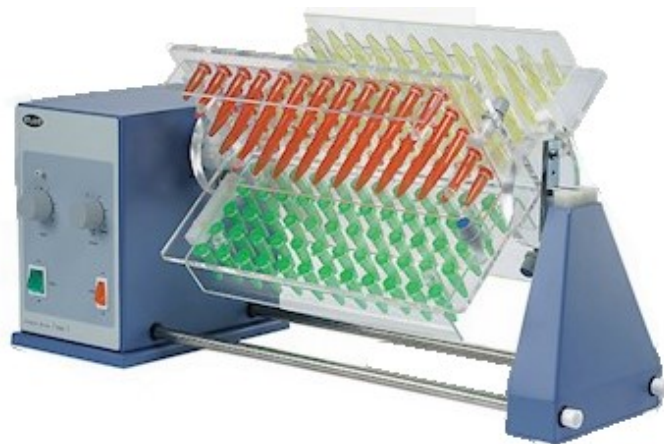


Figure 3-6. Rotating Shaker.

3.3. Setup and Procedure

3.3.1. Brine Softening

The following section describes the process followed to soften the reservoir brine in order to avoid the issues related with divalent cations already explained in the second chapter, Brine softening was performed for all the experiments performed in this thesis as shown in Figure 3-7. First, Auersthal brine was filtered using folded filter paper in order to extract any trace of crude oil still present on it. Then, 10 grams of Dowex® Marathon™ C sodium form were added per every 100 grams of water and the mixture was set in a magnetic stirrer at 400 rpm for 1 hour. Finally, Auersthal/softened was filtered again in order to remove the cation exchanger. Table 3-6 summarizes the brine composition after the softening process.

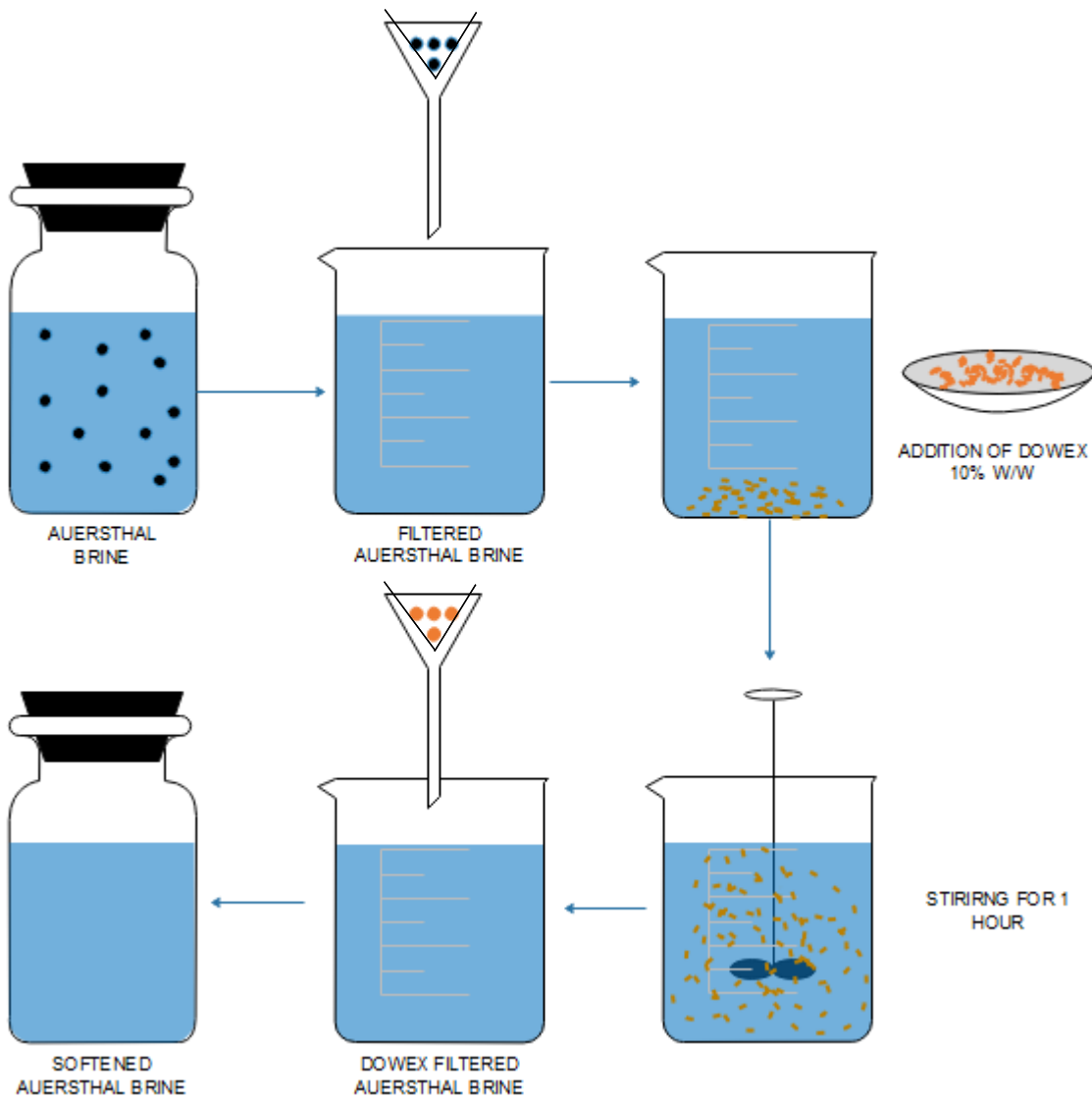


Figure 3-7. Brine Softening Process Description.

Table 3-6: Softened Auersthal Brine Composition

Element	Auersthal Softened Brine
	mg/l
Li	1.41
Na	7814.00
NH4	26.90
K	33.70
Mg	12.90
Ca	12.30
Sr	0.88
Ba	0.29
Fe	-
Total Hardness [dH°]	5.00

3.3.2. Polymer Solution Preparation

Polymeric solutions were prepared following API standards. The preparation of the polymeric solutions can be summarized as follow, see Figure 3-8. First, polymer mother/stock solution was prepared by mixing 0.55 grams of polymer per every 499.45 grams of Auersthal/softened brine (5000 ppm) and stirring the mixture for 5-10 minutes at 600 rpm and then for 2 hours at 300 rpm. Then, the solution was diluted to a desired polymer concentration, between 1000 and 3000 ppm, Finally, diluted solution was set in a magnetic stirrer for 2 hours at 300 rpm.

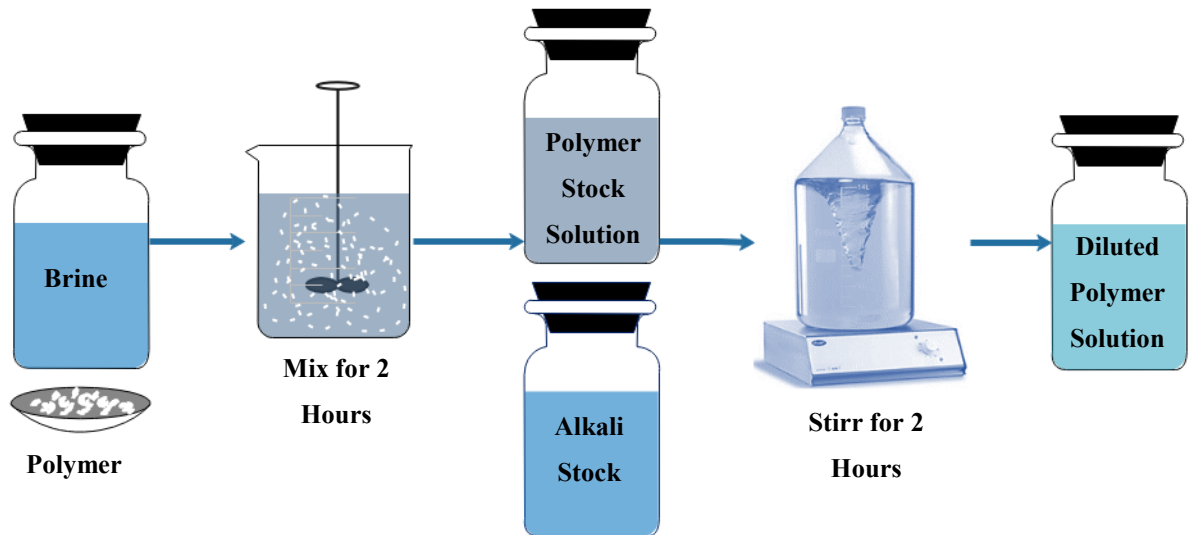


Figure 3-8. Polymer Solution Process Description.

3.3.3. Preliminary Rheological Assessment Description

This section describes the procedure followed during the preliminary rheological assessment, see Figure 3-9. First, polymer solutions were prepared following the procedure explained in Figure 3-8. Following this, diluted solutions were stored for one night in a refrigerator at $\sim 6^{\circ}\text{C}$ in order to avoid any thermal degradation as explained in the second chapter. Then, shear-steady rheological measurements were performed to the diluted solutions at least 3 times using an Anton Paar Physica MCR 301 rheometer with a dual gap geometry. Finally, the obtained data were analyzed in order to determine the ideal polymer solution for the aging and phase experiments.

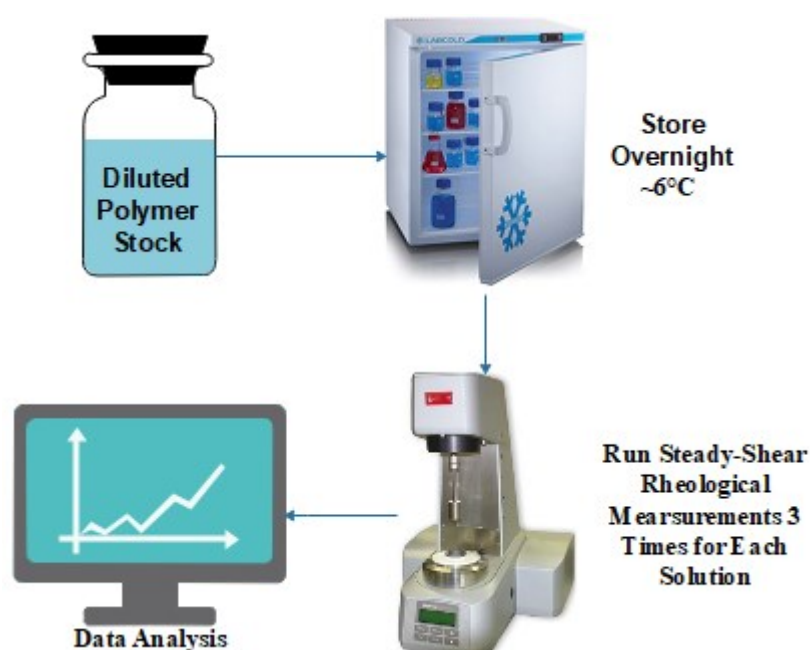


Figure 3-9. Preliminary Rheological Assessment Process Description.

3.3.4. Aging Experiments Description

This section describes the procedure followed during the aging experiments, see Figure 3-10. First, polymer solutions were prepared following the procedure explained in Figure 3-8. Following this, diluted solutions were stored in convection ovens at desired temperatures. Shear-steady rheological measurements were performed to the diluted solutions on a $\sqrt{\text{time}}$ basis using an Anton Paar Physica MCR 301 rheometer with a dual gap geometry. pH and dissolved oxygen were also measured on each measurement day. Finally, the obtained data were analyzed and interpreted in order to study the polymer thermal stability and the effect of temperature, dissolved oxygen, and pH in polymer degradation.

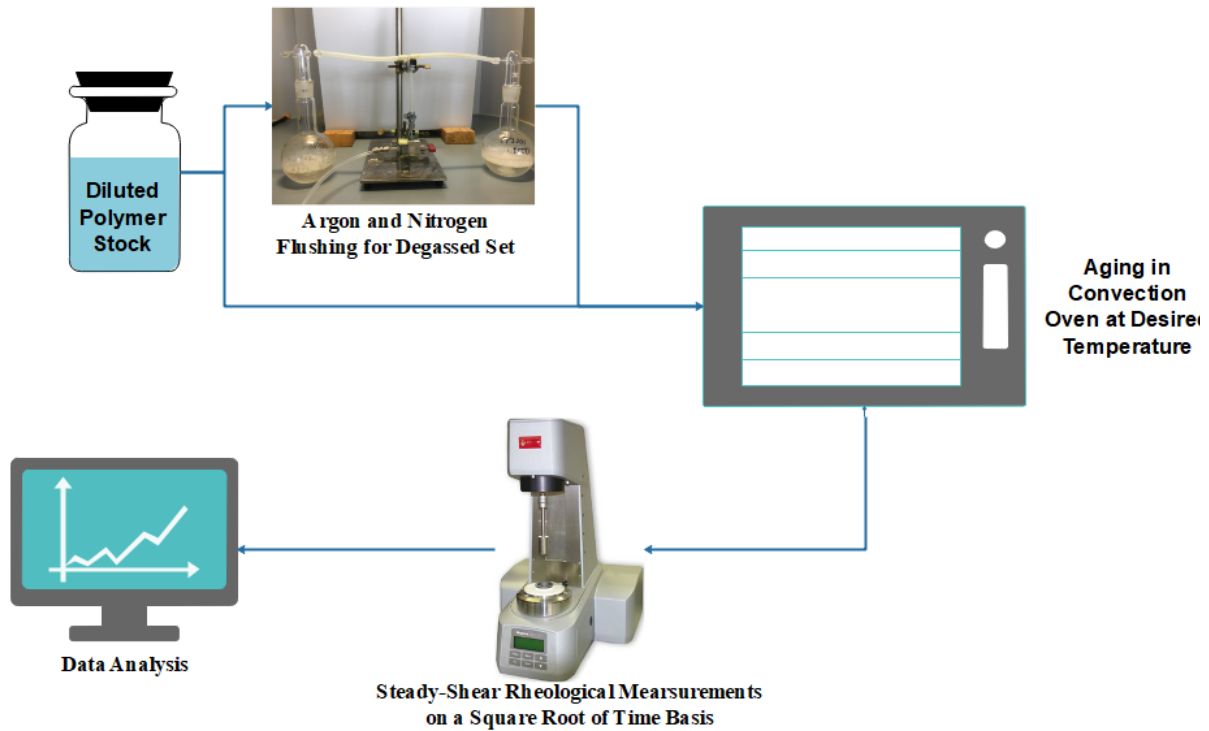


Figure 3-10. Aging Experiments Process Description.

In total, three different sets of polymer solutions were designed to assess polymer thermal stability. The description of the experiment sets is shown in Table 3-7.

Table 3-7: Set of Experiments Defined for the Aging Evaluations

Specifications	Baseline Set	Degassed Set	Temperature Set
Polymers Used	Flopaam 3630 S, Flopaam 5205 VHM, Flopaam 6030		
Temperature (°C)	60	60	50, 70
Rheometer Geometry	Double Gap		
Degassing	No	Argon, Nitrogen	No
Additional Measurements	Dissolved Oxygen, pH		
Polymer Concentration (ppm)	Flopaam 3630 S, Flopaam 5205 → 2000 Flopaam 6030 → 1800		
Alkali Concentration (ppm)	0 and 7500	7500	7500

For the degassed set, an in-house experimental setup was designed to remove the dissolved oxygen from the polymer solution, see Figure 3-11.

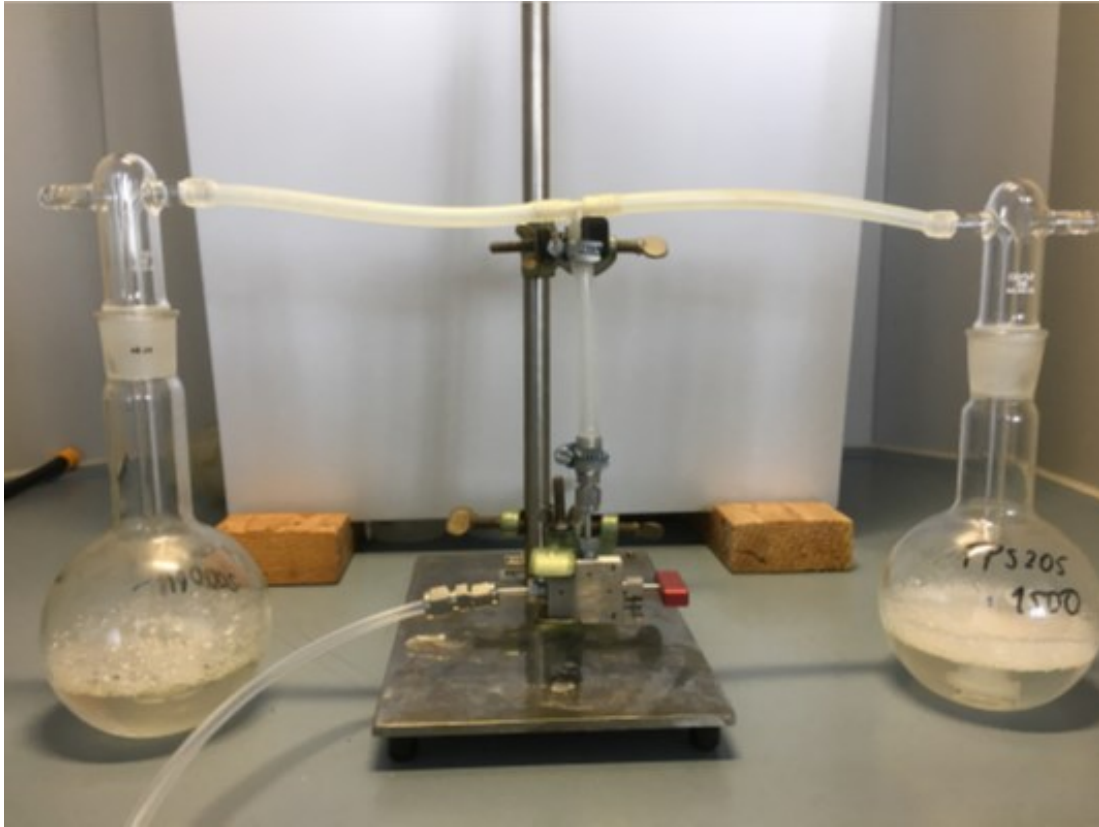


Figure 3-11. Experimental Setup Utilized for Polymer Degassing

3.3.5. Phase Experiments Description

This section describes the procedure followed during phase experiments, see Figure 3-12. Phase experiments were prepared to analyze the effect of both, temperature and polymer presence in the phase behavior of alkali-oil mixtures. First, 10 ml borosilicate pipettes were sealed in the bottom using an oxygenated methane torch. Paralelly, dead oil was surrogated by adding 15 % $\frac{w}{w}$ of cyclohexane to match the viscosity of the oil at reservoir conditions (~ 5 mPa. s), Figure 3-13 shows the shear steady rheological measurements performed on the oil before and after the addition of cyclohexane. Then, polymer and alkali solutions were prepared following the procedure explained in Figure 3-8. Following this, 5 ml of desired A or AP solution and 5 ml of surrogated oil diluted solutions were poured into the pipettes using an Eppendorf repeater. Next, borosilicate pipettes top was sealed using an oxygenated methane torch and let them cool at ambient temperature. Subsequently, sealed pipettes were shaken in a rotator mixer for 24 hours in order to maximize the contact between the alkali-rich solution and the surrogated oil. Finally, the pipettes were stored in convection ovens at desired temperatures.

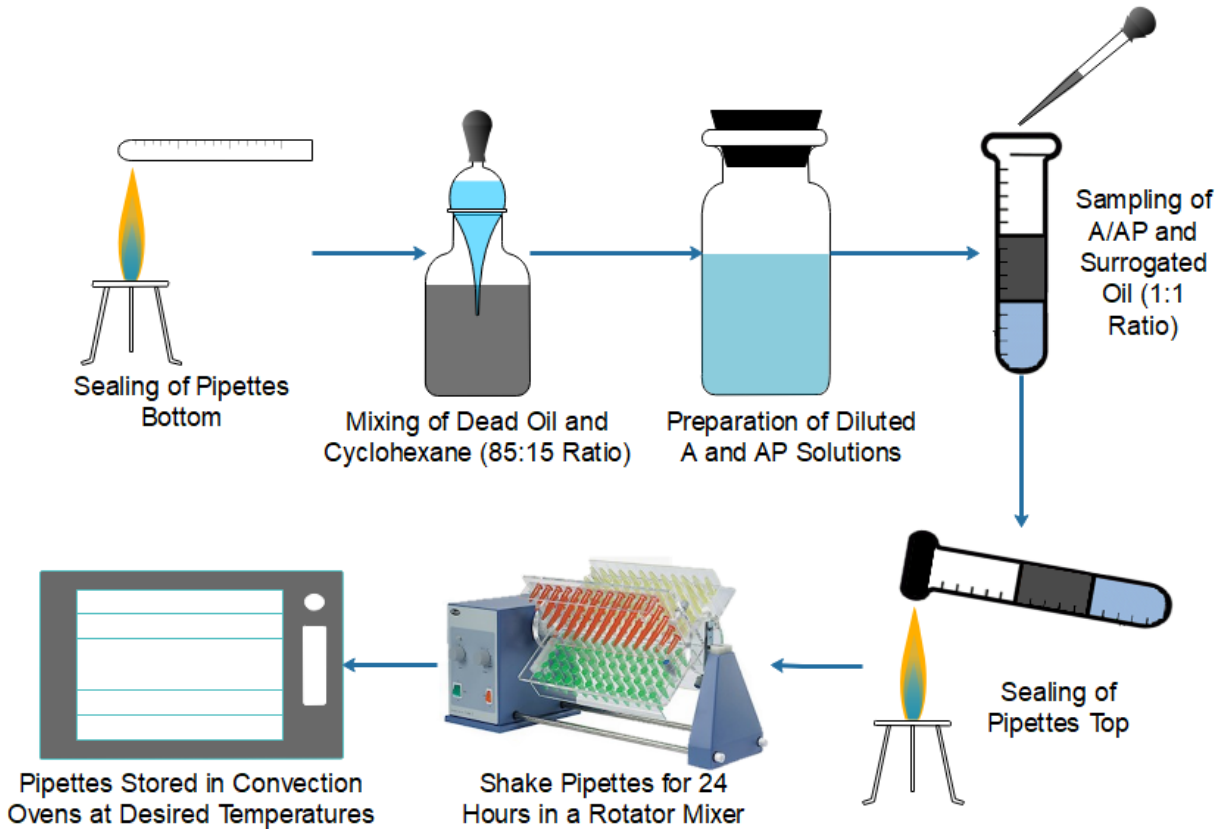


Figure 3-12. Phase Experiments Process Description

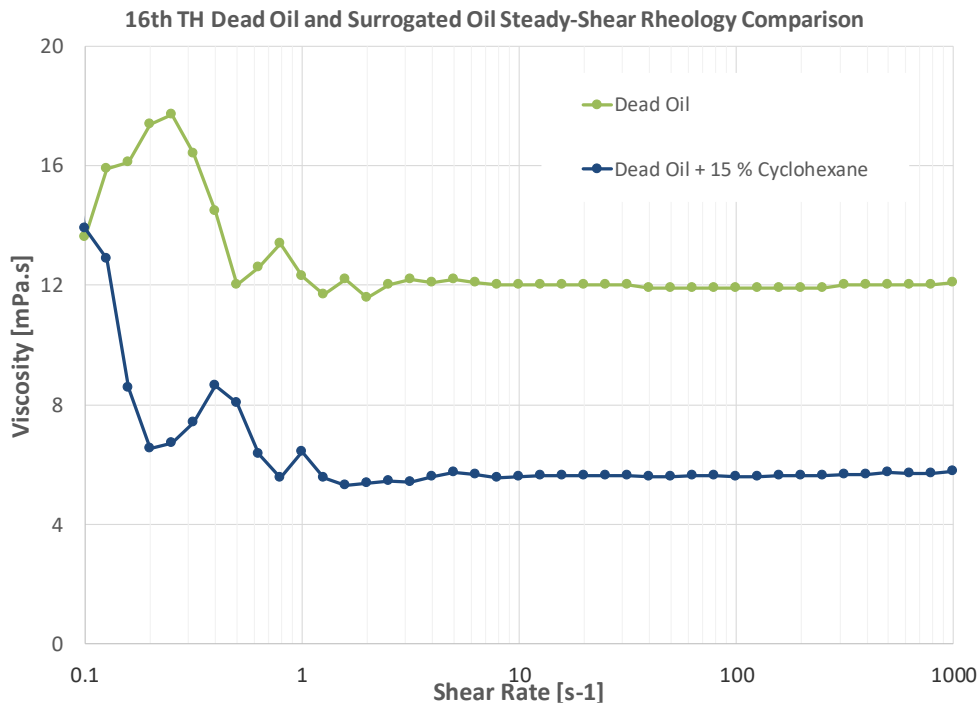


Figure 3-13. Dead Oil and Surrogated Oil Rheological Measurements

In total, three different polymers and three different temperatures were evaluated in the phase experiments. The description of the experiment sets is shown Table 3-8.

Table 3-8: Phase Experiments Description

Specifications	50°C	60°C	70°C
Water Phase	Alkali, Flopaam 3630 S, Flopaam 5205 VHM, Flopaam 6030		
Polymer Concentration	Flopaam 3630 S, Flopaam 5205 → 2000 ppm Flopaam 6030 → 1800 ppm		
Oil Phase	Surrogated (Viscosity matched oil), 15 % w/w Cyclohexane		
Alkali Concentration	6000, 7500, 9000, 10500, 12000, 15000 ppm		
Number of Samples per Concentration	3		

4. EXPERIMENTAL RESULTS

The following chapter describes the performance of the different experiments mentioned in the previous chapter. All reported viscosity values are mean values obtained as an average of all measurements performed on the samples. Data also includes standard deviations showed as error bars in the listed figures.

4.1. Polymer Viscosifying Power

Steady-shear rheological measurements were performed on the three partially hydrolyzed polyacrylamides, showed in Table 3-3, at different polymer concentrations ranging between 1000 ppm and 3000 ppm in order to have a baseline trend of the viscosity behavior for the tested polymers.

Results from preliminary viscosifying power analysis are shown in Figure 4-1 and Figure 4-2. Figure 4-1 shows apparent viscosity for each polymer at different shear rates ranging from 0.1 to 1000 s⁻¹ while Figure 4-2 compares the different apparent viscosities at a given shear rate of 7.96 s⁻¹ which is the closest value to which is considered the normal shear rate at reservoir conditions. All rheological measurements were performed at reservoir temperature (60°C) and were done three times for each sample.

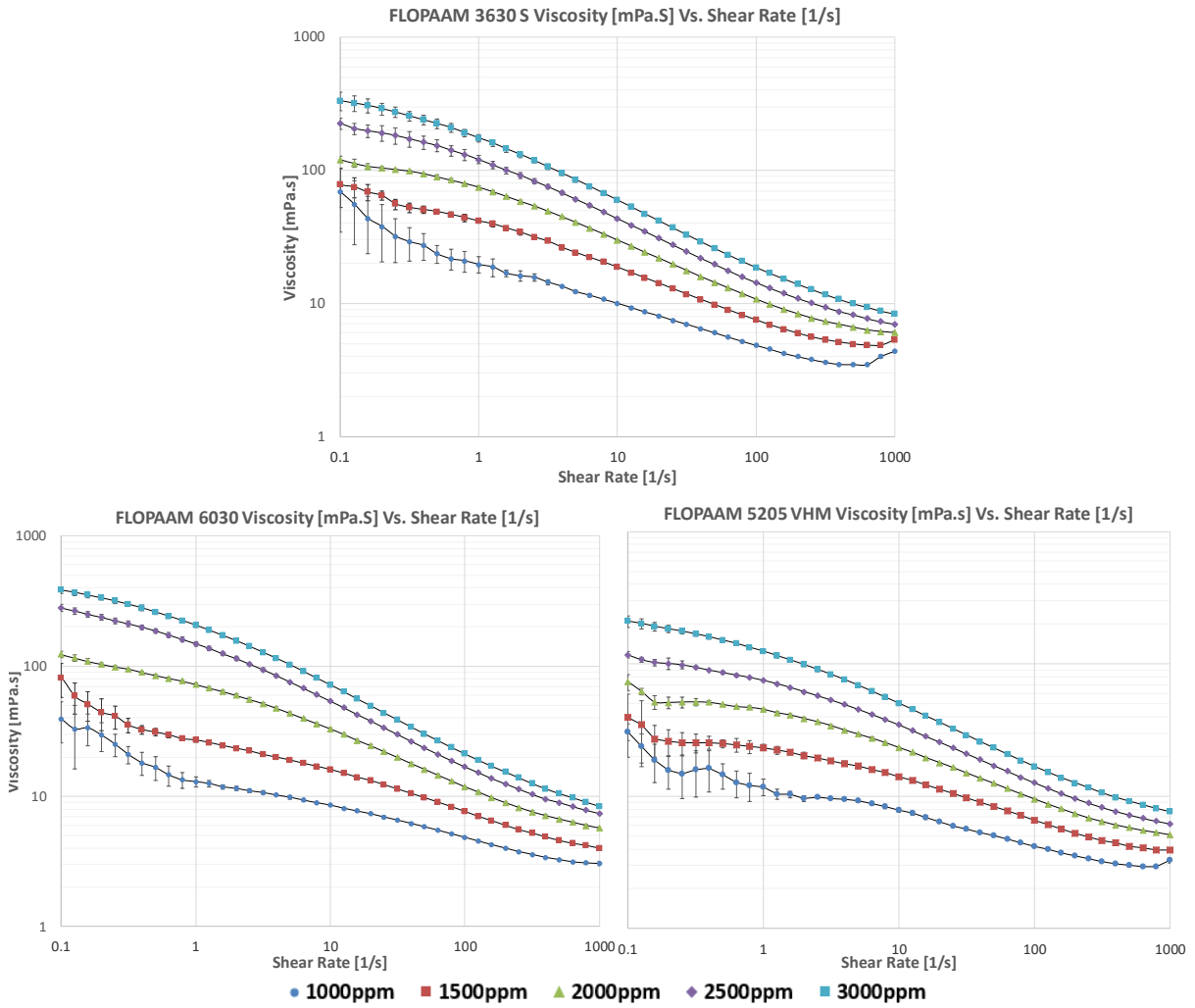


Figure 4-1. Polymers Rheological Behaviour at Different Concentrations

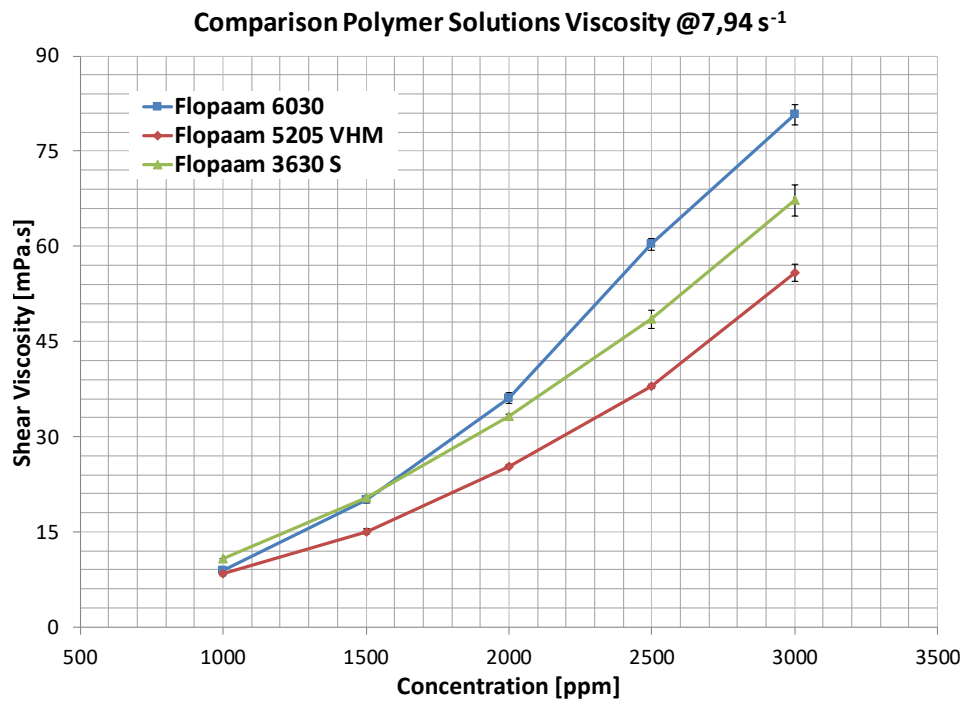


Figure 4-2. Polymers Viscosity Comparison for Different Concentrations at a Shear Rate of 7.94s⁻¹

4.2. Polymer – AP Solutions Comparison

Steady-shear rheological measurements were performed on the three HPAM showed in Table 3-3 at different concentrations ranging between 1000 ppm and 3000 ppm with the addition of an alkali agent (Na₂CO₃) at a fixed concentration of 7500 ppm. This, aiming to understand the effect of alkali presence in the initial viscosity of the studied polymers and with the goal of define polymer concentrations for the aging and phase experiments.

Results from preliminary viscosifying power analysis are shown in Figure 4-3 and Figure 4-4. Figure 4-3 shows apparent viscosity for each polymer at different shear rates ranging from 0.1 s⁻¹ to 1000 s⁻¹ while Figure 4-4 compares the different apparent viscosities at a given shear rate of 7.96 s⁻¹. Moreover, polymer concentrations were defined based on previous laboratory experiments performed by an OMV contractor. Defined concentrations and apparent viscosity values for those concentrations are reported in Table 4-1. All rheological measurements were performed at reservoir temperature (60°C) and were done three times for each sample.

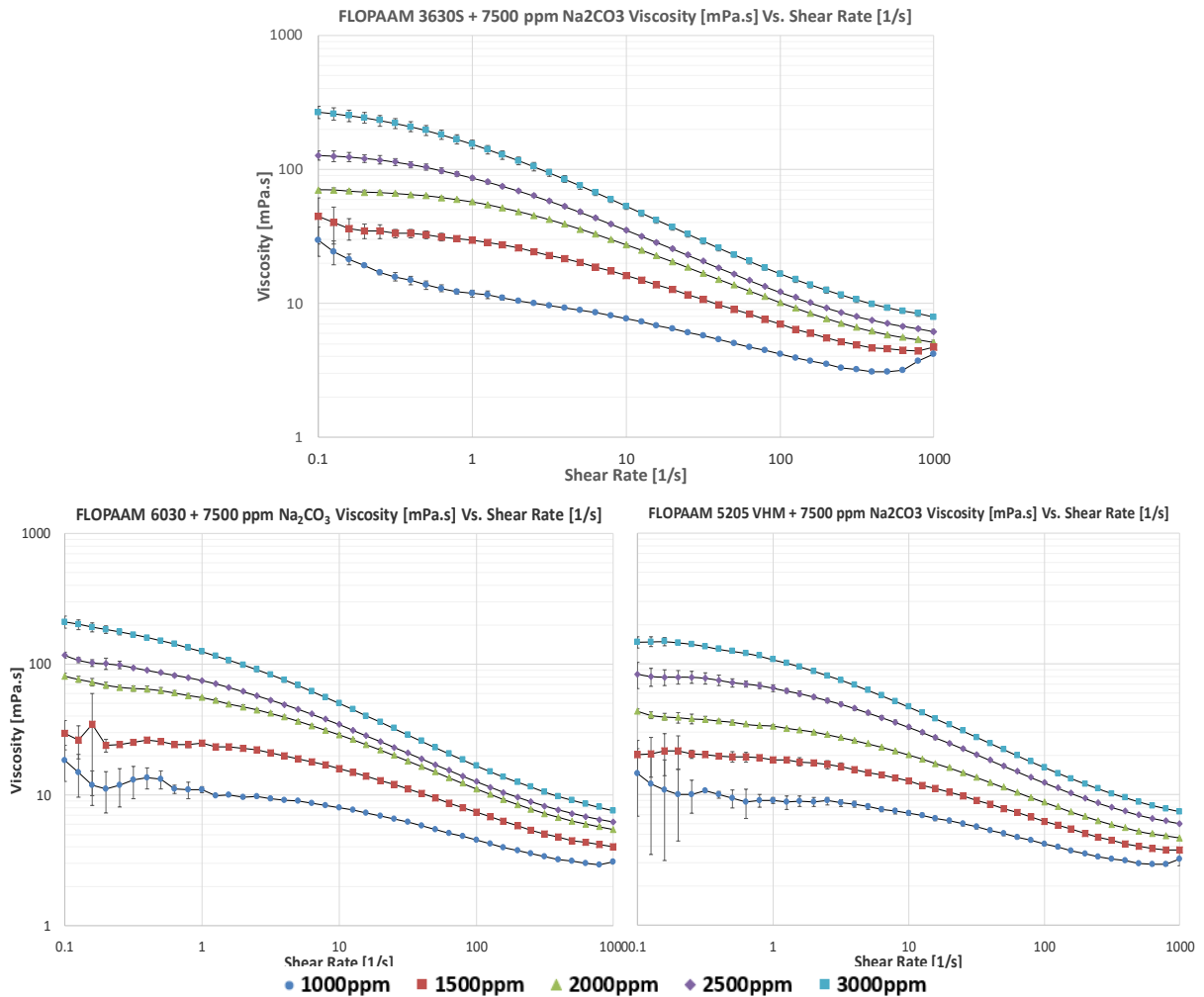


Figure 4-3. Alkali-Polymers Rheological Behaviour at Different Concentrations

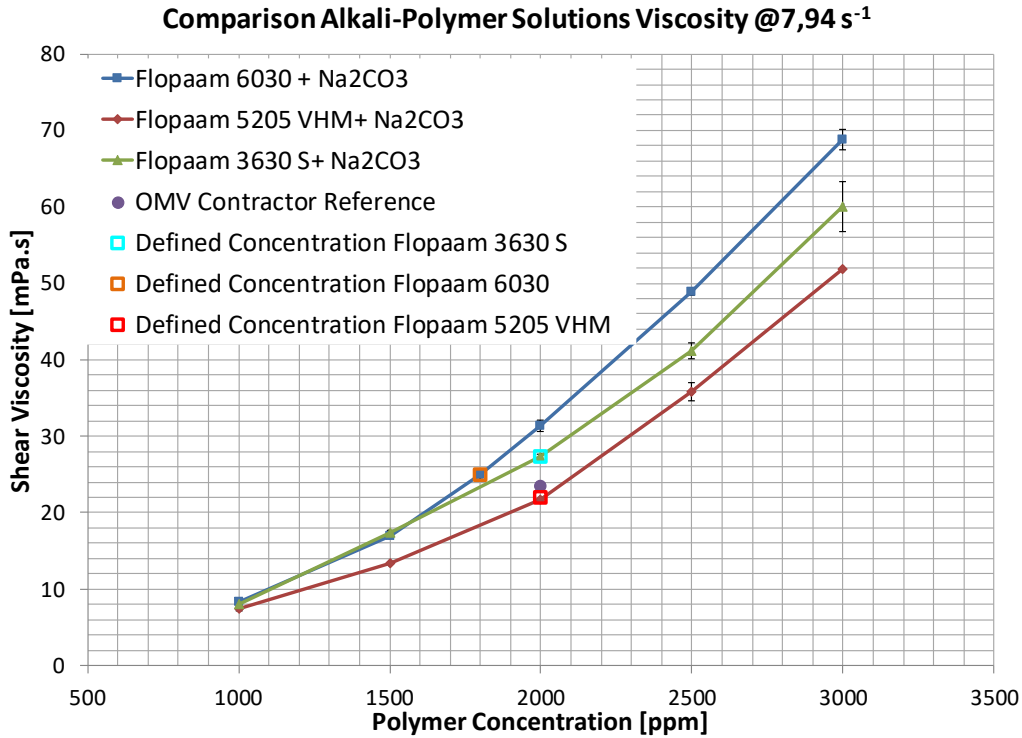


Figure 4-4. Alkali-polymers Viscosity Comparisson for Different Concentrations at a Shear Rate of 7.94s⁻¹

Table 4-1. Polymer Defined Concentrations for Aging and Phase Experiments

	Defined Concentration [ppm]	Viscosity [mPa.s]
Flopaam 3630 S	2000	27.30
Flopaam 6030	1800	24.93
Flopaam 5205 VHM	2000	21.93

4.3. Long-term Stability Assessment

The following sections will report the obtained results from the three different aging experiments explained in detail in section 3.3.4.

4.3.1. Baseline Set

The baseline set was designed to have a reference on how the viscosity of the three different studied polymers behave in the long-term basis. Polymeric solutions at concentrations defined in section 4.2 were prepared without and with the presence of alkali (7500 ppm of Na₂CO₃). Samples were aged at reservoir temperature (60°C). Steady-shear rheology measurements were performed over time roughly on a \sqrt{time} basis. Moreover, pH and dissolved oxygen were also tracked on the same time basis as the rheological measurements were performed. All rheological measurements were performed at reservoir temperature (60°C) and were done three times for each sample.

Results from baseline aging experiments are shown in Table 4-2, Table 4-3 and Figure 4-5. Table 4-2 and Table 4-3 show the changes in time of dissolved oxygen (D.O.) pH respectively. Figure 4-5 shows apparent viscosity over time for each polymer at a shear rate of 7.94 s^{-1} .

Table 4-2. Baseline Dissolved Oxygen Concentration over Time

	Dissolved Oxygen [ppm]							
	Day 1	Day 5	Day 8	Day 16	Day 26	Day 36	Day 49	Day 64
	Flopaam 3630 S	2.7	3.1	2.7	2.6	2.8	2.7	3.2
Flopaam 3630 S + Alkali	2.7	2.6	2.6	2.6	3.4	3.1	3.1	2.9
Flopaam 6030	2.7	2.6	2.7	3.0	2.9	2.8	2.6	2.9
Flopaam 6030 + Alkali	2.6	2.8	2.8	2.7	2.8	2.9	3.1	3.0
Flopaam 5205 VHM	2.6	3.1	2.8	2.6	3.4	3.2	2.9	3.2
Flopaam 5205 VHM + Alkali	2.8	2.6	2.7	2.8	3.2	3.1	3.1	3.0

Table 4-3. Baseline Solutions pH over Time

	pH							
	Day 1	Day 5	Day 8	Day 26	Day 26	Day 36	Day 49	Day 64
	Flopaam 3630 S	8.23	8.33	8.38	8.46	8.65	8.58	8.51
Flopaam 3630 S + Alkali	9.87	9.84	9.72	9.75	9.73	9.71	9.70	9.74
Flopaam 6030	8.27	8.57	8.43	8.55	8.69	8.59	8.52	8.49
Flopaam 6030 + Alkali	9.97	9.84	9.75	9.77	9.72	9.77	9.70	9.79
Flopaam 5205 VHM	8.25	8.39	8.33	8.60	8.77	8.78	8.73	8.50
Flopaam 5205 VHM + Alkali	9.82	9.79	9.73	9.73	9.83	9.75	9.81	9.77

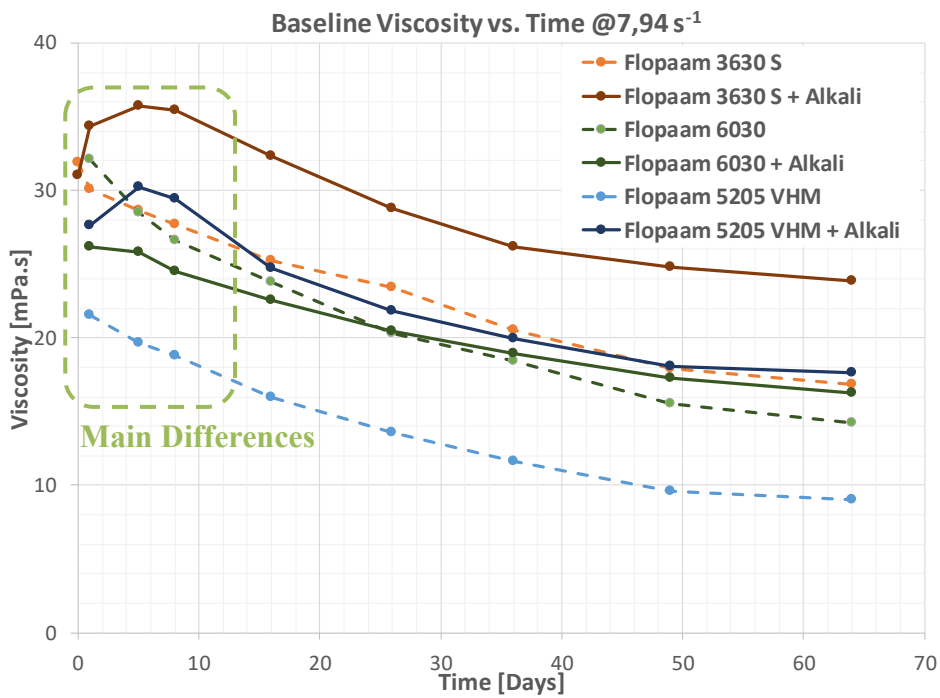


Figure 4-5. Baseline Set Viscosity over Time Comparisson at a Shear Rate of 7.94 s^{-1}

4.3.2. Degassed Set

The degassed set was designed to analyze how the viscosity of the three different studied polymers behave in the long-term basis when the samples were flushed with inert gasses in order to partially remove the dissolved oxygen and try to reproduce the reduced reservoir environment. Polymeric solutions at concentrations defined in section 4.2 were prepared with the presence of alkali (7500 ppm of Na₂CO₃) and were flushed with Nitrogen or Argon (30-45 min). Subsequently, samples were poured in borosilicate glass bottles, sealed quickly and let them age at reservoir temperature (60°C). Steady-shear rheological measurements were performed over time roughly on a \sqrt{time} basis.

The degassing procedure was repeated those days ($\sim\sqrt{t}$) where samples were taken to perform rheological measurements. Dissolved oxygen was measured before and after the Nitrogen or Argon flush to have an idea of how much oxygen was re-dissolved into the solution and how effective the degassing process was. Moreover, solutions pH was also tracked at the same time basis as the rheological measurements were performed. All rheological measurements were performed at reservoir temperature (60°C) and were done three times for each sample.

Results from degassed aging experiments are shown in Table 4-4 and Figure 4-6. Table 4-4 shows the changes in time of solutions pH. Figure 4-6 compares shear viscosity and D.O. over time between the degassed solutions and the alkali-polymer solutions from the baseline set at a shear rate of 7.94 s⁻¹.

Table 4-4. Degassed Solutions pH over Time

	pH								
	Day 0	Day 1	Day 3	Day 10	Day 16	Day 26	Day 36	Day 49	Day 64
Flopaam 3630 S - Nitrogen pH	10.11	9.91	9.99	9.80	9.81	9.79	9.83	9.83	9.83
Flopaam 3630 S - Argon pH	10.12	9.89	9.95	9.85	9.82	9.84	9.90	9.87	9.80
Flopaam 6030 - Nitrogen pH	10.11	9.94	9.81	9.86	9.82	9.82	9.78	9.81	9.73
Flopaam 6030 - Argon pH	10.12	9.99	9.82	9.86	9.82	9.83	9.85	9.76	9.81
Flopaam 5205 VHM - Nitrogen	10.12	9.92	9.83	9.83	9.83	9.84	9.88	9.80	9.83
Flopaam 5205 VHM - Argon	10.11	9.90	9.80	9.79	9.80	9.81	9.76	9.83	9.85

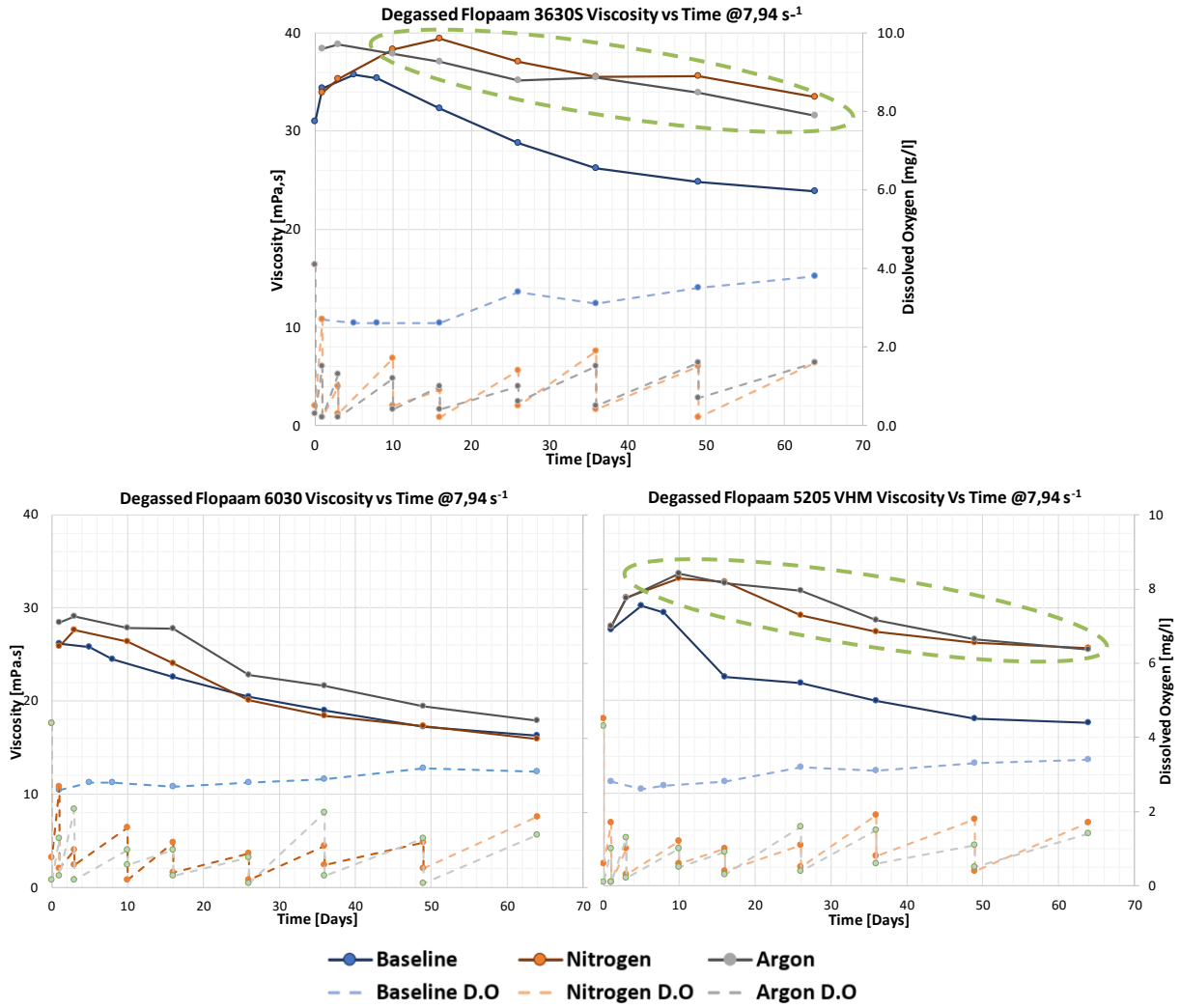


Figure 4-6. Degassed Set Viscosity over Time Comparison at a Shear Rate of 7.94s⁻¹

Validation of Degassing Apparatus

As reported by (Levitt et al., 2011), (Yang and Treiber, 1985), (Rodriguez et al., 2018) among others. Degassed solutions are strongly recommended to be treated using an inert glove-box in order to reproduce the reduced conditions present in the reservoir. To validate the results obtained in this work, the data were compared with a set of experiments that were previously performed externally using Flopaam 3630S, a glove box and a constant dissolved oxygen concentration of 1 ppm as can be seen from Figure 4-7.

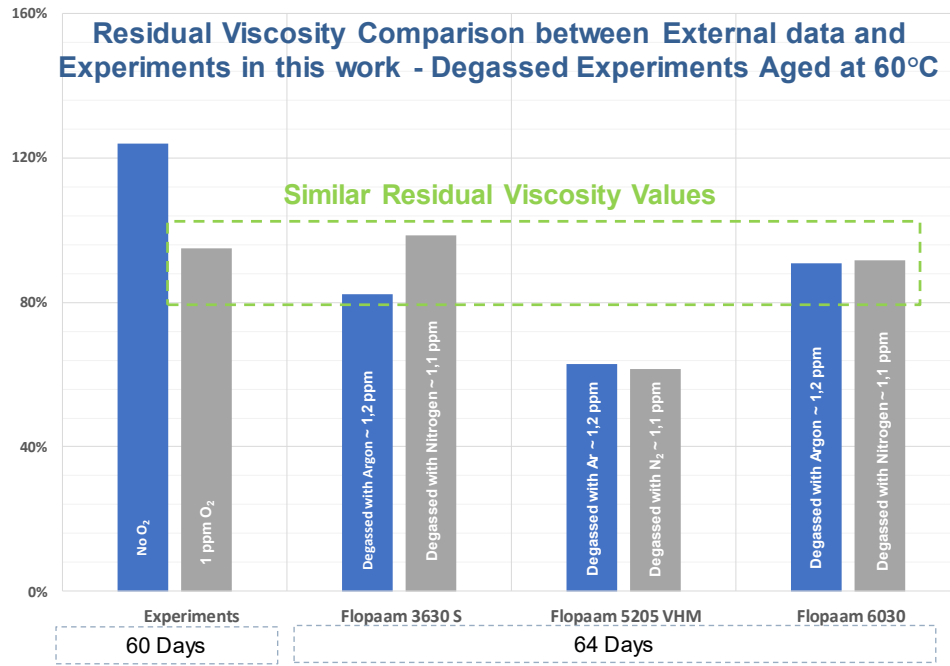


Figure 4-7. Residual Viscosity Comparison between External Experiments and Results from this Work

4.3.3. Temperature Set

Numerous experiments have established the role of temperature in polymer degradation i.e. (Audibert and Argillier, 1995), (Levitt et al., 2011), (Ryles, 1988), among others. The temperature set was designed to have a reference on how the viscosity of the three different studied polymers behave if the aging temperature of the polymeric solutions is different. Alkali-Polymer solutions were prepared at concentrations defined in section 4.2 with 7500 ppm of Na₂CO₃. Samples were aged at 50°C and 70°C. Steady-shear rheology measurements were performed over time roughly on a \sqrt{time} basis. Moreover, as in the other long-term experiments, pH and dissolved oxygen were also tracked on the same time basis as the rheological measurements were performed. All rheological measurements were performed three times on each sample.

Results from baseline aging experiments are shown in Table 4-5 , Table 4-6 and Figure 4-8. Table 4-5 and Table 4-6 show the changes in time of pH and dissolved oxygen respectively. Figure 4-8 shows apparent viscosity over time for each polymer at a shear rate of 7.94 s⁻¹.

Table 4-5. Temperature Dissolved Oxygen Concentration over Time

	Dissolved Oxygen [ppm]						
	Day	Day	Day	Day	Day	Day	Day
	1	4	8	16	26	36	49
Flopaam 3630 S - 50°C	3.2	3.0	3.1	2.9	3.3	3.4	3.2
Flopaam 3630 S - 70°C	3.3	2.6	3.3	3.0	3.2	3.6	3.3
Flopaam 6030 - 50°C	3.3	3.1	3.1	2.8	2.8	3.0	2.9
Flopaam 6030 - 70°C	2.9	3.2	3.1	2.7	2.8	2.7	2.8
Flopaam 5205 VHM - 50°C	3.1	2.8	3.3	3.0	3.2	3.1	2.9
Flopaam 5205 VHM - 70°C	2.9	2.6	3.1	2.9	2.6	2.6	2.7

Table 4-6. Temperature Solutions pH over Time

	pH						
	Day	Day	Day	Day	Day	Day	Day
	1	4	8	16	26	36	49
Flopaam 3630 S - 50°C	9.91	9.83	9.91	9.90	9.89	9.91	9.87
Flopaam 3630 S - 70°C	9.85	9.84	10.01	9.88	9.91	9.85	9.86
Flopaam 6030 - 50°C	9.89	10.06	10.00	9.95	9.90	9.88	9.85
Flopaam 6030 - 70°C	9.87	10.03	9.92	9.83	9.88	9.83	9.85
Flopaam 5205 VHM - 50°C	10.02	10.00	10.04	9.87	9.92	9.88	9.85
Flopaam 5205 VHM - 70°C	9.99	9.87	9.86	9.94	9.95	9.91	9.90

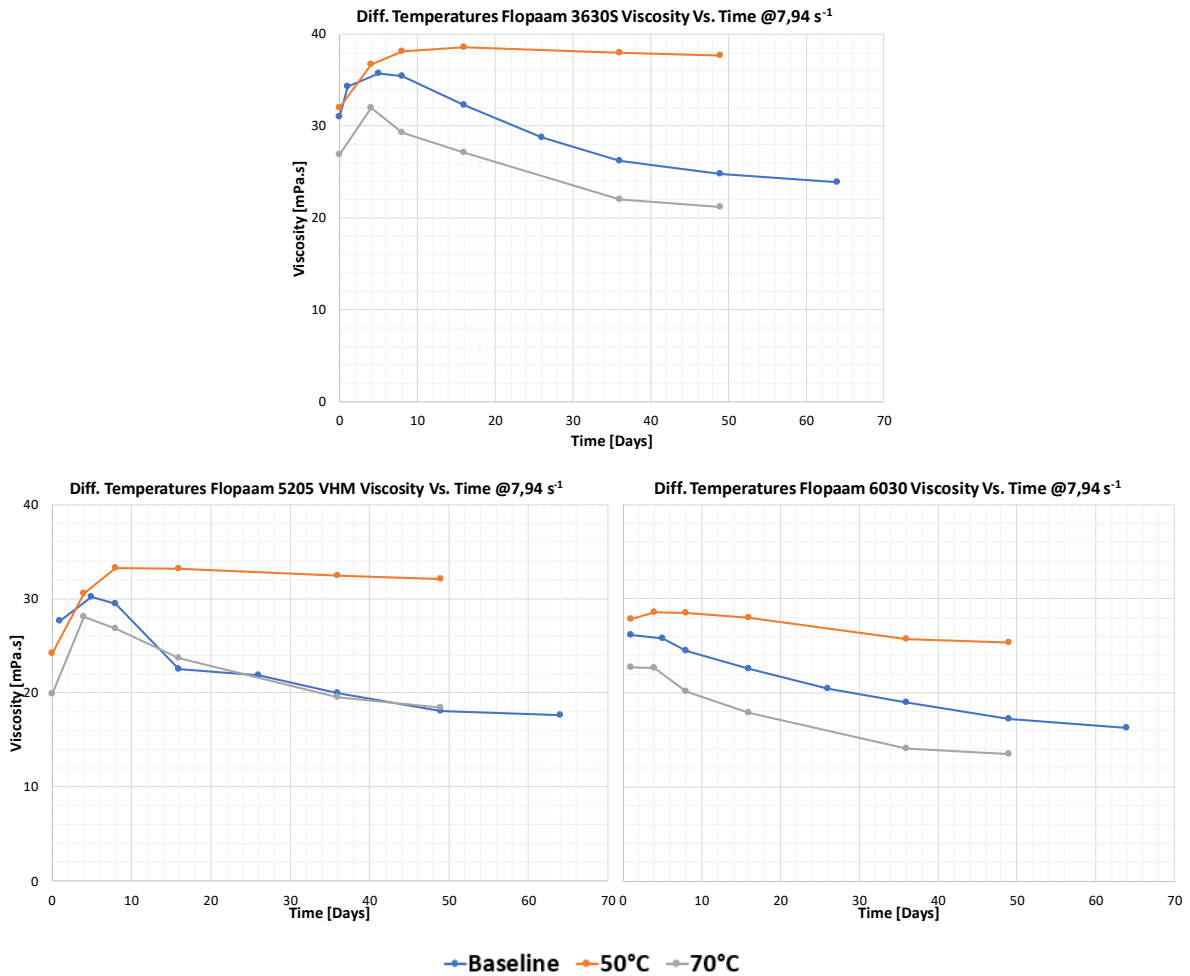


Figure 4-8. Temperature Set Viscosity over Time Comparisson at a Shear Rate of 7.94s⁻¹

4.4. Phase Experiments

The following sections will report the obtained results from all the phases experiments which were explained in detail in section 3.3.5. All reported volumes are mean values from three experiments performed for each alkali concentration.

4.4.1. Emulsions Stability in Time

Phase experiments were continuously monitored, and emulsion volumes read from the pipettes. Emulsion volumes for polymer mixtures were considered to be all the volume above the water level since no clear interface was observed in most experiments, see Figure 4-9. Stability was considered to be reached when emulsion volumes did not change considerably for a period of ten or more days. Reported data include standard deviations shown as error bars.

No Clear Interface



Figure 4-9. Emulsion Volumes Phases Clarification

Results from emulsions stability in time are shown in Figure 4-10, Figure 4-11 and Figure 4-12. Figure 4-10 shows the evolution of emulsion volumes over time for alkali+polymer/oil and alkali/oil mixtures aged at 50°C while Figure 4-11 and Figure 4-12 show the results from the experiments aged at 60°C and 70°C respectively.

Polymer Degradation in High pH Solutions and the Effect of Polymers on the Phase Behavior of Alkali-Oil

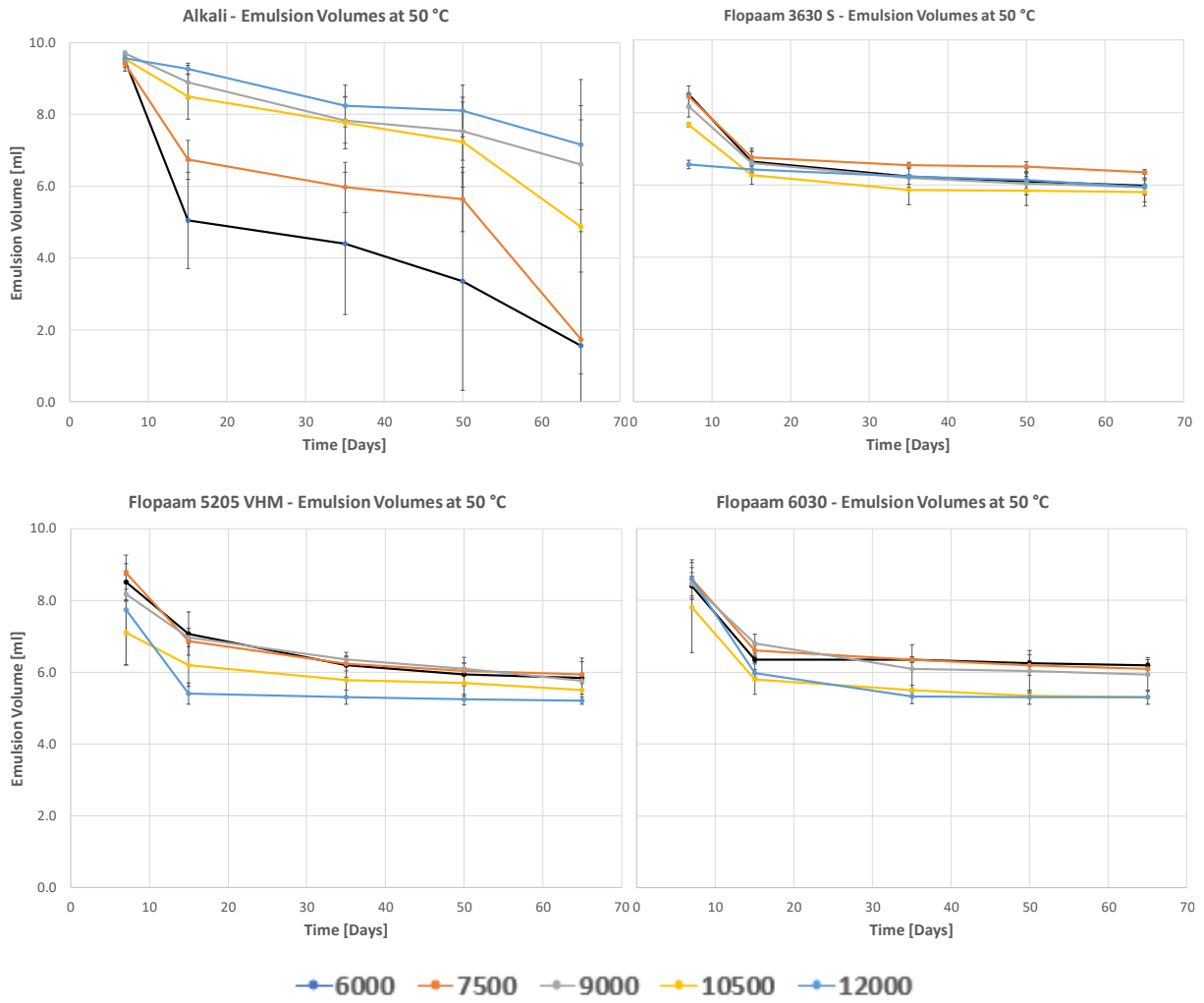


Figure 4-10. Phase Experiments Emulsion Volumes over Time at 50°C

Polymer Degradation in High pH Solutions and the Effect of Polymers on the Phase Behavior of Alkali-Oil

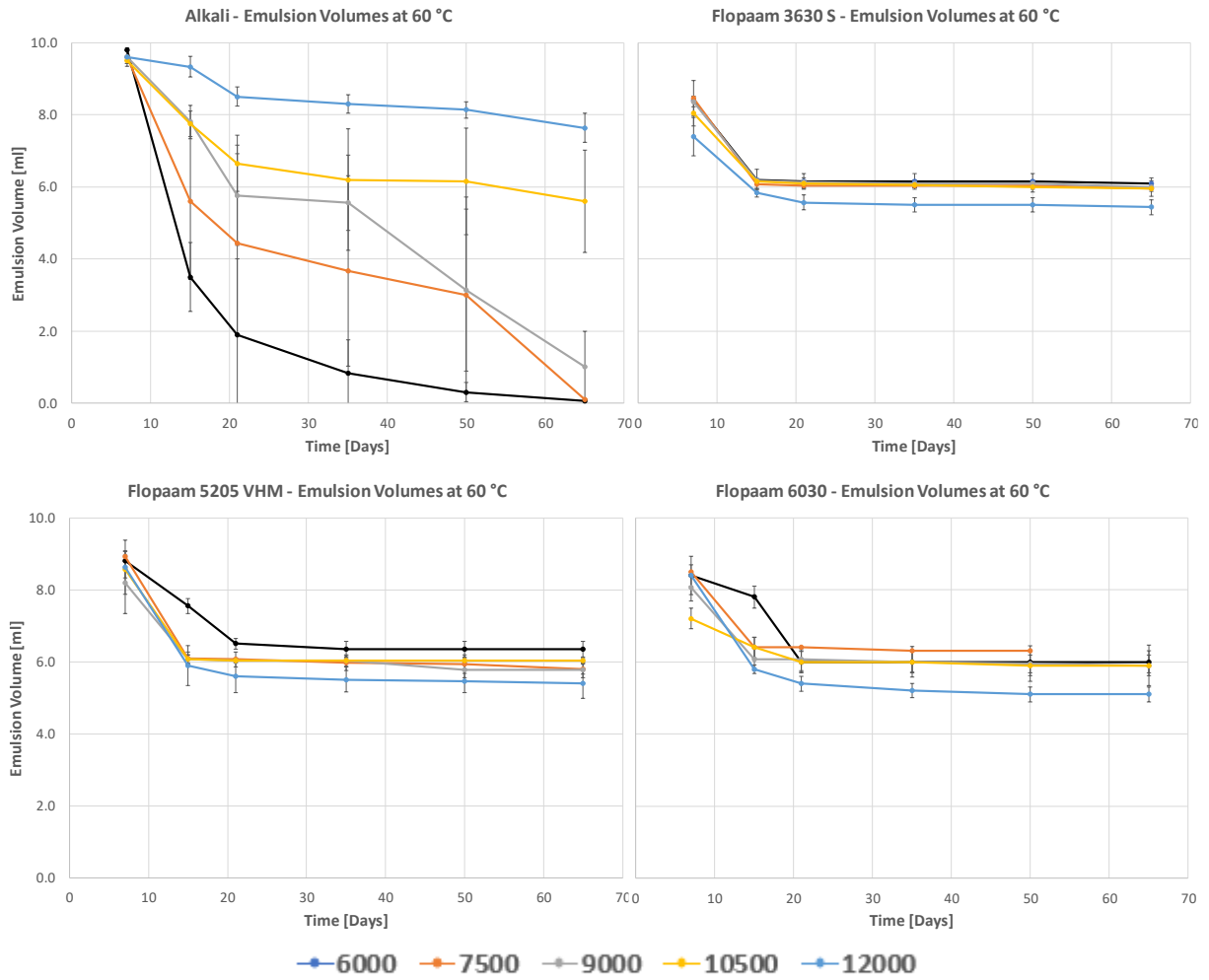


Figure 4-11. Phase Experiments Emulsion Volumes over Time at 60°C

Polymer Degradation in High pH Solutions and the Effect of Polymers on the Phase Behavior of Alkali-Oil

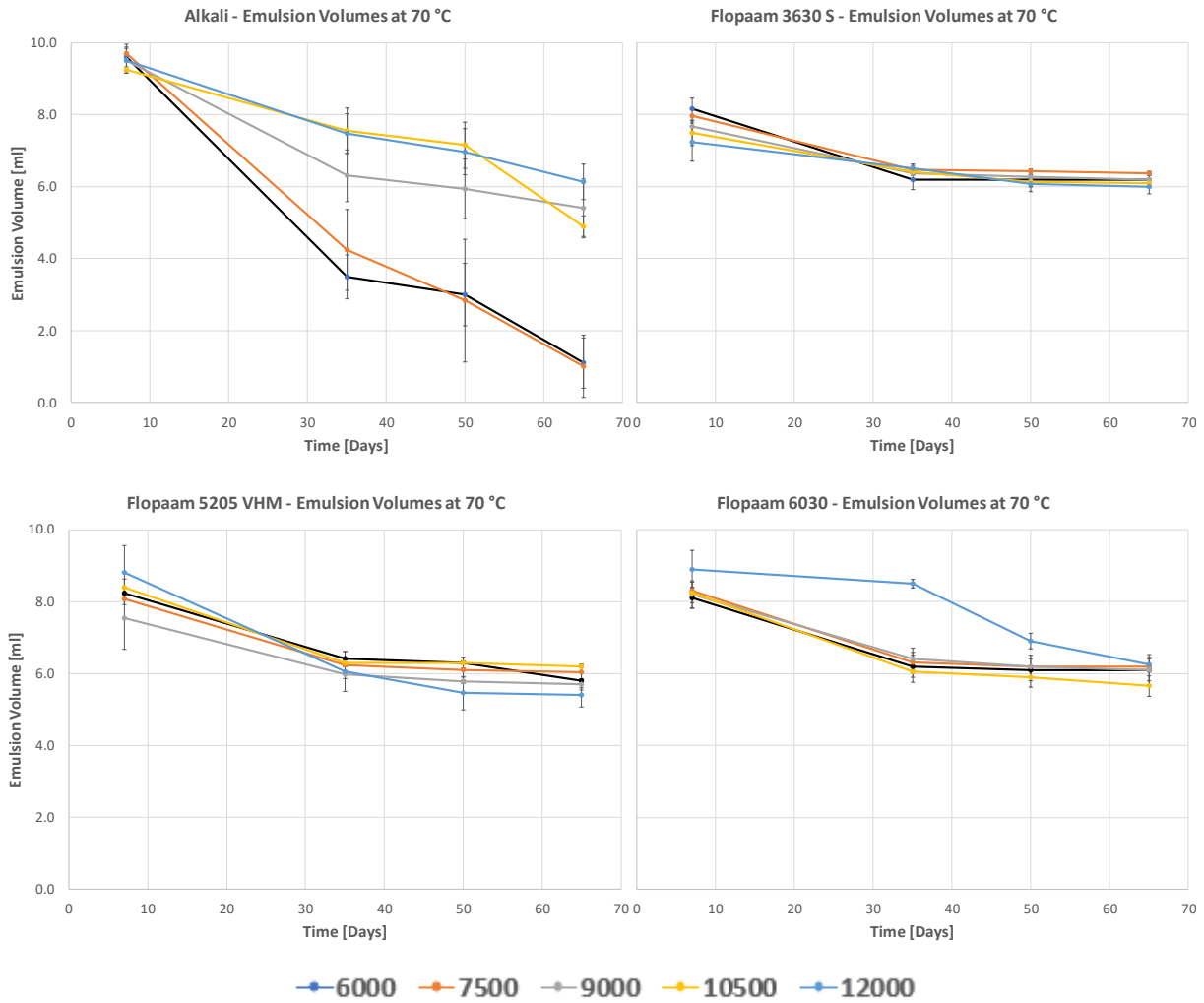


Figure 4-12. Phase Experiments Emulsion Volumes over Time at 70°C

4.4.2. Phase Maps

Phase maps were drawn for the emulsion volumes taken in the last measurement day (day 65) to have an idea of how different concentrations of alkali affect the generated emulsion. Reported volumes are mean values from three experiments performed for each alkali concentration. Instead of using the nomenclature calling the emulsions Type I, II or III as proposed by (Winsor, 1954), this work uses a different nomenclature naming as Emulsion I or Emulsion II. This is because during phase experiments two different emulsions were visually present in most experiments, as shown in Figure 4-13. Emulsion I is an upper dark-brown emulsion that seemed to present low viscosity while Emulsion II is a lower light-brown emulsion that seemed to present high viscosity. The initial appreciation was done by visual eye observation.



Figure 4-13. Phase Maps Nomenclature Clarification

Figure 4-14 shows the phase maps for the alkali+polymer/oil and alkali/oil mixtures aged at 50°C while Figure 4-15 and Figure 4-16 show the results from the experiments aged at 60°C and 70°C respectively.

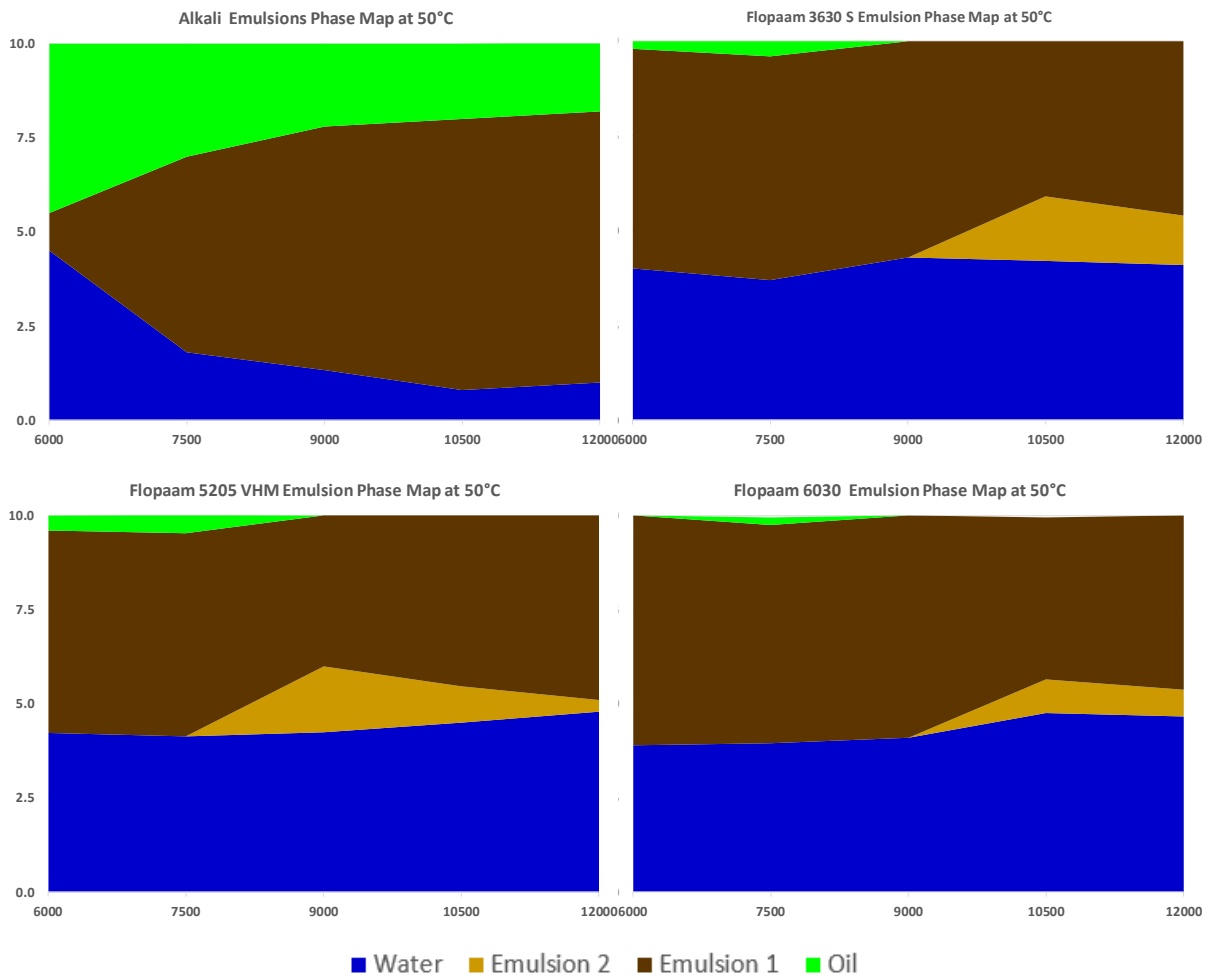


Figure 4-14. Phase Maps at 50°C

Polymer Degradation in High pH Solutions and the Effect of Polymers on the Phase Behavior of Alkali-Oil

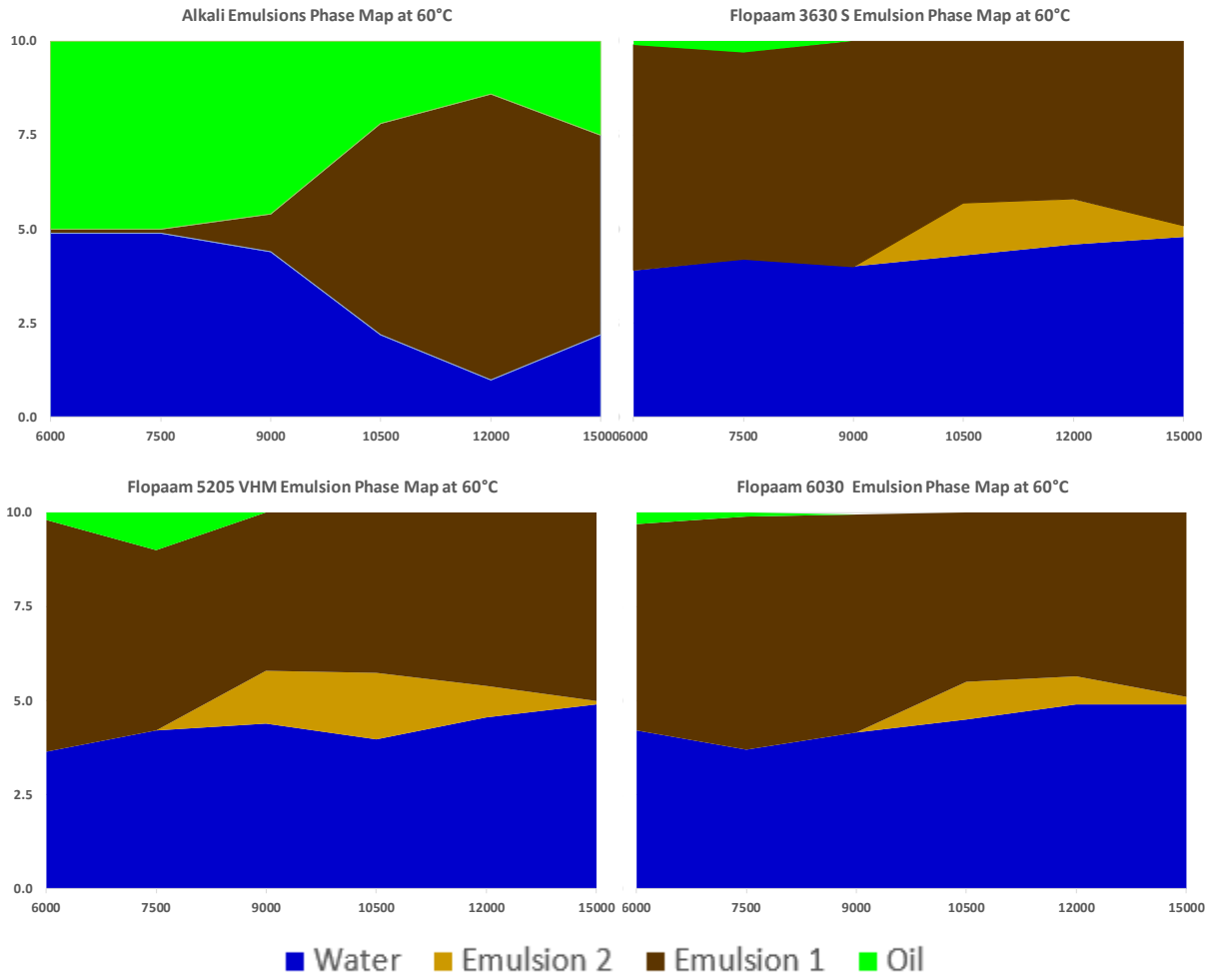


Figure 4-15. Phase Maps at 60°C

Polymer Degradation in High pH Solutions and the Effect of Polymers on the Phase Behavior of Alkali-Oil

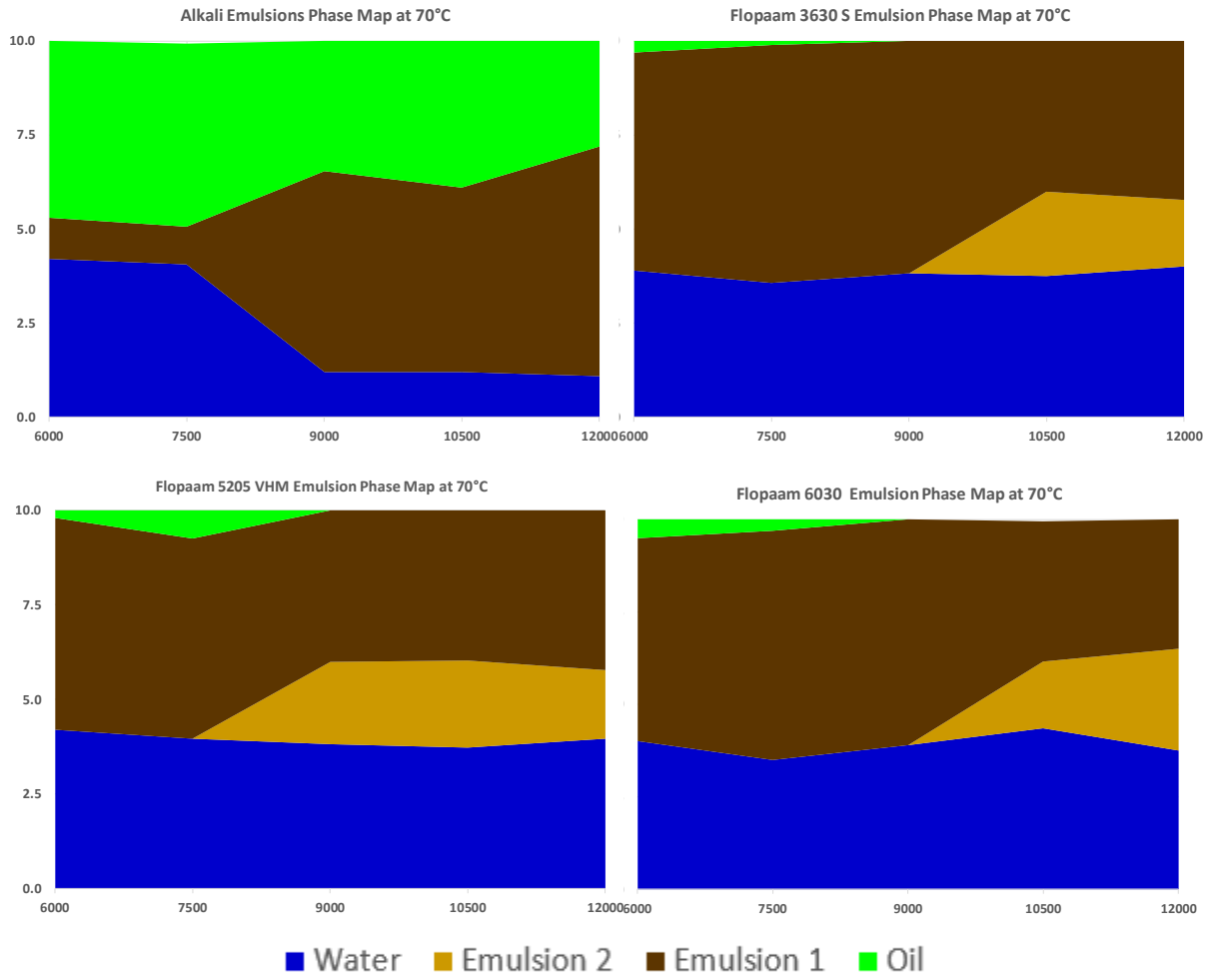


Figure 4-16. Phase Maps at 70°C

5. RESULTS ANALYSIS

5.1. Polymer Viscosifying Power

As seen in Figure 4-1, all polymers show a typical shear thinning behavior. Moreover, it is seen that for low concentration, 1000- to 1500- ppm the standard error is particularly high for low shear rates. This is because it is difficult to assess the shear viscosity for low viscosity fluids at low shear rates. However, this geometry still provides much better-quality data in comparison with other geometries such as cone and plate.

From Figure 4-2 it is possible to conclude that reservoir viscosities 4- to 6- mPa.s. can be reached with a polymer concentration smaller than 1000 ppm. In addition, Flopaam 6030 showed the biggest Viscosifying power followed by Flopaam 3630 S and Flopaam 5205 VHM.

5.2. Polymer – AP Solutions Comparison

As seen in Figure 4-3, the addition of alkali does not affect the general shear thinning behavior of the polymer. Big standard errors are also present for low polymer concentrations 1000- to 1500 ppm, especially for Flopaam 5205 VHM -Figure 4-3c-.

Figure 4-4 shows that as in Polymer only solutions, Flopaam 6030 depicted the highest viscosifying power, followed by Flopaam 3630 S and Flopaam 5205 VHM also for Alkali-Polymer. Moreover, the presence of alkali reduces polymer initial viscosity. At a concentration of 2000 ppm, Alkali-Polymer solutions lead to a reduction of viscosity between 13% and 23% in comparison with Polymer only solutions. The observed viscosity reduction is in agreement with previous studies presented by (Levitt et al., 2011) and (Sheng, 2010). It is assumed that the reduction in polymer viscosity after the addition of the alkali agent is due to particles curling and the increasing in salinity. Having as reference result obtained from previous micromodels/core flooding polymer concentrations were defined for further aging as 1) Flopaam 3630S – 2000ppm, 2) Flopaam 6030 – 1800 ppm, 3) Flopaam 5205 VHM – 2000 ppm as shown in Table 4-1.

5.3. Long-term Stability Assessment

The following sections will analyze the obtained results from the three different aging experiments explained in detail in section 3.3.4.

5.3.1. Baseline Set

As seen in Figure 4-5, there is no evidence of O₂ consumption, as the D.O in all solutions remains roughly constant over time. There are two possible speculative explanations for this

observation. The first one is that the O₂ concentration is in great excess compared to the other chemical compounds that it can react with. The second and most likely to happen is that since the solutions are manipulated at atmospheric conditions -where the O₂ concentration is around -210000 ppm- the oxygen remaining in the storage bottle can dissolve on it until equilibrium is reached. From pH values -Table 4-3- it seems to be an alkali consumption that can be observed with the decreasing of pH for alkali-polymer solutions.

Figure 4-5 shows that AP solutions and P solutions depict a different behavior, especially during the first days of aging. On one hand, AP solutions show an increase in steady-shear viscosity during the first few days and then, a steady decrease approximately after day 10. On the other hand, P solutions present a steady decrease in shear viscosity since day 1. By day 64, all solutions that include alkali depicted a higher shear viscosity than the ones without it. Residual viscosity values for AP solutions is 17 to 25% higher than for P solutions -Table 5-1-. Since the only different parameter between the different solutions was the presence of alkali, it is believed that, as observed by (Levitt et al., 2011) and (Zhang et al., 2017) presence of alkali enhances viscosity at first due to the increase in hydrolysis. As a final note, contrary to the baseline assessment in which Flopaam 6030 depicted the highest viscosifying power for both AP and P solutions, the long-term baseline assessment shows that Flopaam 3630 S is the Polymer that has the best performance in untreated solutions (no O₂ removal).

Table 5-1. Baseline Residual Viscosities Comparison

	FP 3630	FP 3630 + A	FP 6030	FP 6030 + A	FP 5205	FP5205 + A
Mean Residual Viscosity [mPa.s]	16,80	23,90	14,70	16,30	9,00	17,60
Residual Viscosity	52%	77%	45%	62%	40%	63%

5.3.2. Degassed Set

Results from Table 4-4 showed that degassed solutions have very similar pH values in comparison with alkali-polymer solutions from the Baseline Set. This means that as expected, the addition of an inert gas does not affect the solution pH. The reduction of pH over time is believed to be due to alkali consumption.

It can be observed from Figure 4-6 that dissolved oxygen plays a major role in the long-term stability of polymer solutions. Results presented here are in good agreement with similar observations reported by (Yang and Treiber, 1985), (Moradi-Araghi and Doe, 1987), (Luo et al., 2006), (Seright and Skjevrak, 2015) and (Jouenne et al., 2017). This is also reflected in the viscosity differences between the treated and untreated (baseline) solutions. Degassed solutions

have performed better in terms of final shear viscosity when compared to the baseline experiments in five (5) out of six (6) samples. Treated solutions performed much better for Flopaam 3630 S (Figure 4-6a) and Flopaam 5205 VHM (Figure 4-6b) -highlighted in green dashed circle- than for Flopaam 6030 (Figure 4-6c). After 64 days, treated solutions depicted a viscosity value 30-35 % higher than untreated solutions for the Flopaam 3630 S and 44-45 % higher for the Flopaam 5205 VHM. In the case of Flopaam 6030, treated and untreated solutions depicted roughly the same final viscosity. Moreover, as seen in Figure 4-6, both Nitrogen and Argon have similar performances in the degassing process -similar dissolved oxygen and viscosity values over time-.

Validation of Degassing Apparatus

Even though as seen in Figure 4-6 the D.O. concentration cannot be constant during time since oxygen trapped in the storage bottle is able to re-dissolve in the solution, Figure 4-7 shows that after implementing the degassing approach presented in this work for 60 days, residual viscosity values for Argon-degassed and Nitrogen-degassed solutions are 82% and 99%. On the other hand, External experiments show a 95%. This means that the degassing approach used in this work can be used as an economic alternative to perform long-term stability assessments in partially reduced conditions (1ppm). However, if experiments have to be carried out under anaerobic conditions (<10ppb) the implementation of a glove-box is necessary since the presented approach cannot reach those dissolved oxygen levels.

5.3.3. Temperature Set

From Table 4-5 and Table 4-6 is possible to observe similar behaviour as the ones seen in the Baseline and Degassed sets. In the case of D.O -Table 4-5- it remains nearly constant over time. These results go against the fact that temperature affects the kinetics of reaction and that lower and higher oxygen consumption was expected for solutions aged at 50- and 70-°C respectively. However, as explained in section 5.3.1 the oxygen remaining in the storage bottle can dissolve on it until equilibrium is reached -around 3 ppm-.

Polymers present different behavior under different temperatures owing to the kinetics of reactions (Pashaei et al., 2010). Therefore, Temperature effect was evaluated using the exponential decay model by (Seright and Henrici, 1990) -Table 5-2-.

$$\ln \frac{\eta - \eta_{Brine}}{\eta_{initial} - \eta_{Brine}} = - \frac{time}{\tau} \quad (5.1)$$

Where $\eta_{initial}$ is the first polymer viscosity measurement, η is the measured polymer viscosity at a given time, and η_{Brine} is the brine viscosity, τ is the decay constant, which is the time for the specific viscosity ($\mu-\mu_s$) to fall to $\frac{(\mu_0-\mu_s)}{e}$. By calculating the decay constant is possible to estimate the half time period ($T_{1/2}$) of a polymer solution by Equation 3.

$$T_{1/2} = \ln 2 * \tau \tag{5.2}$$

Table 5-2: Long-Term Temperature Set Results

Temperature	Polymer Name	Viscosity [mPa.s]					τ [days ⁻¹]	$T_{1/2}$ [days]
		Day 1	Day 8	Day 16	Day 36	Day 49		
50°C	Flopaam 3630 S	32.0	38.2	38.6	38.0	37.7	1359	942
60°C	Flopaam 3630 S	31.0	35.4	32.3	26.2	24.8	110	76
70°C	Flopaam 3630 S	26.9	29.3	27.1	22.0	21.2	106	74
50°C	Flopaam 6030	27.9	28.5	28.0	25.7	25.4	331	230
60°C	Flopaam 6030	26.2	24.5	22.6	25.7	17.3	109	75
70°C	Flopaam 6030	22.7	20.2	17.9	14.1	13.5	86	60
50°C	Flopaam 5205 VHM	24.2	33.3	33.2	32.1	32.5	1091	756
60°C	Flopaam 5205 VHM	27.7	29.5	22.6	20.0	18.1	85	59
70°C	Flopaam 5205 VHM	19.9	26.9	23.7	19.5	18.5	102	71

From Table 5-2, it can be seen that the aging temperature affects the polymer stability drastically. All studied polymers present similar half-life times when aged at 60°C and 70°C. However, when solutions are aged at 50°C Flopaam 3630S and Flopaam 5205 VHM 4- and 2.5-times higher half-life values than Flopaam 6030.

From Figure 4-8 it can be pointed out that degradation is similar between solutions aged at 60 °C and 70 °C -comparable trends in Figure 4-8a,b,c- and much less drastic for solutions aged at 50°C. In fact, half-life time for solutions aged at 60°C and 70°C range within 59 and 75 days, while solutions aged at 50°C show a half-time life that ranges within 230 and 942 days. This is due to the lower kinetics of reactions at a lower temperature.

5.4. Phase Experiments

The following sections discuss the results obtained from all the phases experiments which were explained in detail in section 3.3.5.

5.4.1. Emulsions Stability in Time

Two main observations can be pointed out from Figure 4-10, Figure 4-11 and Figure 4-12 despite of the aging temperature. First, alkali mixtures take longer to stabilize than mixtures

that contain additional Polymer. Regardless of the aging temperature, for alkali mixtures, changes in volume are observed even after 65 days of aging. On the other hand, for alkali-polymer mixtures, there are no considerable changes in volume after day 15. Also, for alkali mixtures, an increase in alkali concentration increases also the amount of generated emulsion. On the other hand, for polymer mixtures, this volume seems to be almost constant despite of the alkali concentration.

5.4.2. Phase Maps

From phase maps are shown in Figure 4-14, Figure 4-15 and Figure 4-16 it can be deduced that regardless the temperature, the largest generated emulsion for alkali mixtures is obtained at 12000 ppm of Na_2CO_3 . Emulsion volume increases with an increase of alkali until 12000 ppm. When using higher concentrations than that, generated emulsion decreases as seen in Figure 4-14a. This reduction in emulsion volumes is in agreement with results previously obtained by (Leitenmueller et al., 2018).

In addition, the adding of polymer affect the phase behavior of the mixtures drastically. In alkali solutions, especially at higher concentrations (9000+ ppm of Na_2CO_3) at least half of the brine volume partitions into the emulsion phase. On the other hand, all solutions in which polymer is present, only 20% (1ml) of brine partition into the emulsion phase despite of the alkali concentration. Finally, no evident volumetric differences are observed among the different polymers (Figure 4-14b,c,d, Figure 4-15b,c,d and Figure 4-16b,c,d). In all cases, only emulsion I is formed at low concentrations while at higher alkali concentrations emulsion 2 is formed.

6. CONCLUSIONS

Based on the obtained results and observations made from the experiments presented in this work, the following conclusions can be drawn:

- Flopaam 3630 S and Flopaam 5205 VHM showed promising long-term stability results in all experiments that included alkali-polymer solutions, especially in the degassed set in which residual viscosities values ranged between 82% to 99% and 90% to 91% respectively. Moreover, no major behaviors were observed in the degassed set regardless the inert gas used.
- Low oxygen concentrations are necessary to be able to reproduce the reduced reservoir environment; otherwise, results might be misleading or too pessimistic.
- The apparatus used for the degassed set can be used as an economic alternative to perform long-term stability assessments.
- The presence of polymers strongly affects the phase behavior of alkali-oil solutions. It reduces the amount of water that can partition into the emulsion phase. Moreover, no major differences in phase behavior were observed for the three studied polymers.
- Long-term stability tests showed that presence of alkali enhances polymer residual viscosity (η/η_0 , corrected by η_{brine}), with residual viscosity decreasing once temperature is increased. However, viscosities at a given time were higher for solutions in presence of alkali compared to those without. Solutions aged at 50°C depicted 20-30% higher residual viscosity when compared to the solutions aged at 70°C. Degassing of solutions with argon/nitrogen enhances polymer long-term stability.
- Results showed that degassed solutions had 25% higher residual viscosity than untreated solutions and were in a good match with previous results performed by an external company in an anaerobic environment. Complementarily, phase experiments depicted that presence of polymer reduces water solubility. Once alkali concentration was increased a 3-phase system, mainly described as macro-emulsion was observed, microemulsions were only described by visual/light-through observations, since droplet-size measurements were not available.

7. REFERENCES

- ABIDIN, A. Z., PUSPASARI, T. & NUGROHO, W. A. 2012. Polymers for Enhanced Oil Recovery Technology. *Procedia Chemistry*, 4, 11-16.
- AJITH, J. & ANIMESH, R. 1994. Phase Behavior and Properties of a Microemulsion in the Presence of NaCl. *Langmuir*, 10, 2084-2087.
- ALAM, M. W. & TIAB, D. 1985. Mobility Control of Caustic Flood. Society of Petroleum Engineers.
- ALVARADO, V. & MANRIQUE, E. 2010. *Enhanced oil recovery: field planning and development strategies*, Gulf Professional Publishing.
- ÅSEN, S. M., STAVLAND, A., STRAND, D. & HIORTH, A. 2018. An Experimental Investigation of Polymer Mechanical Degradation at cm and m Scale. *SPE Improved Oil Recovery Conference*. Tulsa, Oklahoma, USA: Society of Petroleum Engineers.
- AUDIBERT, A. & ARGILLIER, J. F. 1995. Thermal stability of sulfonated polymers. *SPE International Symposium on Oilfield Chemistry*. San Antonio, Texas: Society of Petroleum Engineers.
- AUSTAD, T., MATRE, B., MILTER, J., SÆVAREID, A. & ØYNO, L. 1998. Chemical flooding of oil reservoirs 8. Spontaneous oil expulsion from oil- and water-wet low permeable chalk material by imbibition of aqueous surfactant solutions. *Colloids and Surfaces A: Physicochemical and Engineering Aspects*, 137, 117-129.
- BENNETT, K. E., DAVIS, H. T., MACOSKO, C. W. & SCRIVEN, L. E. 1981. Microemulsion Rheology: Newtonian and Non-Newtonian Regimes. *SPE Annual Technical Conference and Exhibition*. San Antonio, Texas: Society of Petroleum Engineers.
- BOURREL, M. & SCHECHTER, R. S. 1988. *Microemulsions and related systems: formulation, solvency, and physical properties*, Editions Technip.
- CANTER, N. H., ROBBINS, M. L. & BAKER, E. G. 1982. Polymer-microemulsion complexes for the enhanced recovery of oil. Google Patents.

- CHEN, Z., SUN, W. & YANG, H. 1999. Mechanistic study of alkaline–polymer flooding in Yangsanmu Field. 29, 237-240.
- CHON, B. H. & YU, B.-H. 2001. *The Effect of Changing Mobility Ratio on Displacement Efficiency in Polymer Flooding*.
- CLEMENS, T., DECKERS, M., KORNBERGER, M., GUMPENBERGER, T. & ZECHNER, M. 2013. Polymer Solution Injection - Near Wellbore Dynamics and Displacement Efficiency, Pilot Test Results, Matzen Field, Austria. *EAGE Annual Conference & Exhibition incorporating SPE Europec*. London, UK: Society of Petroleum Engineers.
- CLIFFORD, P. J. & SORBIE, K. S. 1985. The Effects of Chemical Degradation on Polymer Flooding. *SPE Oilfield and Geothermal Chemistry Symposium*. Phoenix, Arizona: Society of Petroleum Engineers.
- DAVIS, J. A., GOGARTY, W. B., JONES, S. C. & TOSCH, W. C. 1968. Oil Recovery Using Micellar Solutions. *Drilling and Production Practice*. New York, New York: American Petroleum Institute.
- DAVISON, P. & MENTZER, E. 1982. Polymer Flooding in North Sea Reservoirs. *Society of Petroleum Engineers Journal*, 22, 353-362.
- DE-QIANG, S., PU-HA, Y. & YAN-LI, L. J. O. C. 1993. ALKALINE AND POLYMER INTERACTIONS IN RELATION TO INTERFACIAL TENSIONS BETWEEN ALKALINE/POLYMER SOLUTIONS AND CRUDE OIL [J]. 1, 009.
- FORTENBERRY, R., KIM, D. H., NIZAMIDIN, N., ADKINS, S., ARACHCHILAGE, G. W. P. P., KOH, H. S., WEERASOORIYA, U. & POPE, G. A. 2015. Use of Cosolvents To Improve Alkaline/Polymer Flooding. *SPE Journal*, 20, 255-266.
- GAILLARD, N., GIOVANNETTI, B., LEBLANC, T., THOMAS, A., BRAUN, O. & FAVERO, C. 2015. Selection of Customized Polymers to Enhance Oil Recovery from High Temperature Reservoirs. *SPE Latin American and Caribbean Petroleum Engineering Conference*. Quito, Ecuador: Society of Petroleum Engineers.
- GAO, S., LI, H. & LI, H. 1995. Laboratory Investigation of Combination of Alkaline-Surfactant-Polymer for Daqing EOR. *SPE Reservoir Engineering*, 10, 194-197.

- GBADAMOSI, A. O., KIWALABYE, J., JUNIN, R. & AUGUSTINE, A. 2018. A review of gas enhanced oil recovery schemes used in the North Sea. *Journal of Petroleum Exploration and Production Technology*.
- GOGARTY, W. B. & TOSCH, W. C. 1968. Miscible-Type Waterflooding: Oil Recovery with Micellar Solutions. *Journal of Petroleum Technology*, 20, 1407-1414.
- GREEN, D. W. & WILLHITE, G. P. 1998. *Enhanced Oil Recovery*, Henry L. Doherty Memorial Fund of AIME, Society of Petroleum Engineers.
- GREGORY, S. D. 1984. Determination of Molecular Weights and Molecular Weight Distribution of Polyacrylamides. *SPE Annual Technical Conference and Exhibition*. Houston, Texas: Society of Petroleum Engineers.
- GRUENWALDER, M., POELLITZER, S. & CLEMENS, T. 2007. Assisted and Manual History Matching of a Reservoir with 120 Wells, 58 Years Production History and Multiple Well Re-Completions. *EUROPEC/EAGE Conference and Exhibition*. London, U.K.: Society of Petroleum Engineers.
- GUO, H. 2017. How to Select Polymer Molecular Weight and Concentration to Avoid Blocking in Polymer Flooding? *SPE Symposium: Production Enhancement and Cost Optimisation*. Kuala Lumpur, Malaysia: Society of Petroleum Engineers.
- HEALY, R. N., REED, R. L. & STENMARK, D. G. 1976. Multiphase Microemulsion Systems. *Society of Petroleum Engineers Journal*, 16, 147-160.
- JOHNSON, C. E., JR. 1976. Status of Caustic and Emulsion Methods. *Journal of Petroleum Technology*, 28, 85-92.
- JOUENNE, S., ANFRAY, J., CORDELIER, P. R., MATEEN, K., LEVITT, D., SOUILEM, I., MARCHAL, P., LEMAITRE, C., CHOPLIN, L., NESVIK, J. & WALDMAN, T. 2015. Degradation (or Lack Thereof) and Drag Reduction of HPAM Solutions During Transport in Turbulent Flow in Pipelines. *Oil and Gas Facilities*, 4, 80-92.
- JOUENNE, S., CHAKIBI, H. & LEVITT, D. 2018. Polymer Stability After Successive Mechanical-Degradation Events. *SPE Journal*, 23, 18-33.

- JOUENNE, S., KLIMENKO, A. & LEVITT, D. 2017. Polymer Flooding: Establishing Specifications for Dissolved Oxygen and Iron in Injection Water. *SPE Journal*, 22, 438-446.
- KANG, W. 2001. Study of chemical interactions and drive mechanisms in Daqing ASP flooding. *Petroleum Industry Press*.
- KAZEMI NIA KORRANI, A., SEPEHRNOORI, K. & DELSHAD, M. 2016. A Mechanistic Integrated Geochemical and Chemical-Flooding Tool for Alkaline/Surfactant/Polymer Floods. *SPE Journal*, 21, 32-54.
- KIENBERGER, G. & FUCHS, R. 2006. A Case History of the Matzen Field - 16th Torton: A Story of Success! Where is the End? *SPE Europec/EAGE Annual Conference and Exhibition*. Vienna, Austria: Society of Petroleum Engineers.
- KONG, B. 1996. Aging effect at high temperature on HPAM solution behavior. 3, 7-12.
- KRUMRINE, P. & FALCONE, J. J. 1987. *Beyond Alkaline Flooding: Design of Complete Chemical Systems*.
- LAKE, L. W. 1989. *Enhanced oil recovery*, Prentice Hall.
- LEITENMUELLER, V., TOUMI, O., HOFSTAETTER, H. & CLEMENS, T. 2018. Microemulsion Formation & Its Effect on Rheology Using Carbonate-Based Alkalies for AP or ASP Floods in the Matzen Field. *SPE EOR Conference at Oil and Gas West Asia*. Muscat, Oman: Society of Petroleum Engineers.
- LEVITT, D., KLIMENKO, A., JOUENNE, S., PASSADE-BOUPAT, N., CORDELIER, P., MOREL, D. & BOURREL, M. 2016. Designing and Injecting a Chemical Formulation for a Successful Off-Shore Chemical EOR Pilot in a High-Temperature, High-Salinity, Low-Permeability Carbonate Field. *SPE Improved Oil Recovery Conference*. Tulsa, Oklahoma, USA: Society of Petroleum Engineers.
- LEVITT, D. & POPE, G. A. 2008. Selection and Screening of Polymers for Enhanced-Oil Recovery. *SPE Symposium on Improved Oil Recovery*. Tulsa, Oklahoma, USA: Society of Petroleum Engineers.

- LEVITT, D. B., POPE, G. A. & JOUENNE, S. 2011. Chemical Degradation of Polyacrylamide Polymers Under Alkaline Conditions. *SPE Reservoir Evaluation & Engineering*, 14, 281-286.
- LÜFTENEGGER, M. & CLEMENS, T. 2017. Chromatography Effects in Alkali Surfactant Polymer Flooding. *SPE Europec featured at 79th EAGE Conference and Exhibition*. Paris, France: Society of Petroleum Engineers.
- LUO, J., LIU, Y. & ZHU, P. 2006. Polymer solution properties and displacement mechanisms. *Enhanced oil recovery–polymer flooding*. Petroleum Industry Press, Beijing, 1-72.
- MORADI-ARAGHI, A. & DOE, P. H. 1987. Hydrolysis and Precipitation of Polyacrylamides in Hard Brines at Elevated Temperatures. *SPE Reservoir Engineering*, 2, 189-198.
- MULLER, G., FENYO, J. C. & SELEGNY, E. 1980. High molecular weight hydrolyzed polyacrylamides. III. Effect of temperature on chemical stability. *Journal of Applied Polymer Science*, 25, 627-633.
- NEEDHAM, R. B. & DOE, P. H. 1987. Polymer Flooding Review. *Journal of Petroleum Technology*, 39, 1503-1507.
- NELSON, R. C., LAWSON, J. B., THIGPEN, D. R. & STEGEMEIER, G. L. 1984. Cosurfactant-Enhanced Alkaline Flooding. *SPE Enhanced Oil Recovery Symposium*. Tulsa, Oklahoma: Society of Petroleum Engineers.
- PASHAEI, S., SIDDARAMAIAH & SYED, A. A. 2010. Thermal degradation kinetics of polyurethane/organically modified montmorillonite clay nanocomposites by TGA. *Journal of Macromolecular Science, Part A: Pure and Applied Chemistry*, 47, 777-783.
- POELLITZER, S., GRUENWALDER, M., KIENBERGER, G. & CLEMENS, T. 2008. How to Optimise Oil Recovery after almost 60 Years of Production from the Matzen Field, Austria. *Europec/EAGE Conference and Exhibition*. Rome, Italy: Society of Petroleum Engineers.
- POTTS, D. E. & KUEHNE, D. L. 1988. Strategy for Alkaline/Polymer Flood Design With Berea and Reservoir-Rock Corefloods. *SPE Reservoir Engineering*, 3, 1143-1152.

- PUERTO, M. C., HIRASAKI, G. J., MILLER, C. A., REZNIK, C., DUBEY, S., BARNES, J. R. & VAN KUIJK, S. 2015. Effects of Hardness and Cosurfactant on Phase Behavior of Alcohol-Free Alkyl Propoxylated Sulfate Systems. *SPE Journal*, 20, 1145-1153.
- PULS, C., CLEMENS, T., SLEDZ, C., KADNAR, R. & GUMPENBERGER, T. 2016. Mechanical Degradation of Polymers During Injection, Reservoir Propagation and Production - Field Test Results 8 TH Reservoir, Austria. *SPE Europec featured at 78th EAGE Conference and Exhibition*. Vienna, Austria: Society of Petroleum Engineers.
- PYE, D. J. 1964. Improved Secondary Recovery by Control of Water Mobility. *Journal of Petroleum Technology*, 16, 911-916.
- RODRIGUEZ, L., ANTIGNARD, S., GIOVANNETTI, B., DUPUIS, G., GAILLARD, N., JOUENNE, S., BOURDAROT, G., MOREL, D., ZAITOUN, A. & GRASSL, B. 2018. A New Thermally Stable Synthetic Polymer for Harsh Conditions of Middle East Reservoirs. *SEG/AAPG/EAGE/SPE Research and Development Petroleum Conference and Exhibition*. Abu Dhabi, UAE: Society of Exploration Geophysicists.
- RUDIN, J., BERNARD, C., WASAN, D. T. J. I. & RESEARCH, E. C. 1994. Effect of added surfactant on interfacial tension and spontaneous emulsification in alkali/acidic oil systems. 33, 1150-1158.
- RYLES, R. G. 1988. Chemical Stability Limits of Water-Soluble Polymers Used in Oil Recovery Processes. *SPE Reservoir Engineering*, 3, 23-34.
- SAGI, A. R., PUERTO, M. C., BIAN, Y., MILLER, C. A., HIRASAKI, G. J., SALEHI, M., THOMAS, C. P. & KWAN, J. T. 2013. Laboratory Studies for Surfactant Flood in Low-Temperature, Low-Salinity Fractured Carbonate Reservoir. *SPE International Symposium on Oilfield Chemistry*. The Woodlands, Texas, USA: Society of Petroleum Engineers.
- SALAGER, J. L., MORGAN, J. C., SCHECHTER, R. S., WADE, W. H. & VASQUEZ, E. 1979. Optimum Formulation of Surfactant/Water/Oil Systems for Minimum Interfacial Tension or Phase Behavior. *Society of Petroleum Engineers Journal*, 19, 107-115.

- SERIGHT, R. & SKJEVRAK, I. 2015. Effect of Dissolved Iron and Oxygen on Stability of Hydrolyzed Polyacrylamide Polymers. *SPE Journal*, 20, 433-441.
- SERIGHT, R. S. & HENRICI, B. J. 1990. Xanthan Stability at Elevated Temperatures. *SPE Reservoir Engineering*, 5, 52-60.
- SHENG, D., YANG, P. & LIU. 1994. Effect of alkali-polymer interaction on the solution properties. 21, 81-85.
- SHENG, J. 2010. *Modern Chemical Enhanced Oil Recovery: Theory and Practice*.
- SHENG, J. J. 2011a. Chapter 5 - Polymer Flooding. In: SHENG, J. J. (ed.) *Modern Chemical Enhanced Oil Recovery*. Boston: Gulf Professional Publishing.
- SHENG, J. J. 2011b. Chapter 10 - Alkaline Flooding. In: SHENG, J. J. (ed.) *Modern Chemical Enhanced Oil Recovery*. Boston: Gulf Professional Publishing.
- SHENG, J. J. 2011c. Chapter 11 - Alkaline-Polymer Flooding. In: SHENG, J. J. (ed.) *Modern Chemical Enhanced Oil Recovery*. Boston: Gulf Professional Publishing.
- SHENG, J. J. 2011d. Chapter 13 - Alkaline-Surfactant-Polymer Flooding. In: SHENG, J. J. (ed.) *Modern Chemical Enhanced Oil Recovery*. Boston: Gulf Professional Publishing.
- SHENG, J. J. 2015. Status of surfactant EOR technology. *Petroleum*, 1, 97-105.
- SHENG, J. 2017. Critical review of alkaline-polymer flooding. *Journal of Petroleum Exploration and Production Technology*, 7, 147-153.
- SHUPE, R. D. 1981. Chemical Stability of Polyacrylamide Polymers. *Journal of Petroleum Technology*, 33, 1513-1529.
- SKAUGE, A. & FOTLAND, P. 1990. Effect of Pressure and Temperature on the Phase Behavior of Microemulsions. *SPE Reservoir Engineering*, 5, 601-608.
- SORBIE, K. S. 1991. *Polymer-improved oil recovery / K.S. Sorbie*, Glasgow : Boca Raton, Fla, Blackie ; CRC Press.

- SUNIGA, P. T., FORTENBERRY, R. & DELSHAD, M. 2016. Observations of Microemulsion Viscosity for Surfactant EOR Processes. *SPE Improved Oil Recovery Conference*. Tulsa, Oklahoma, USA: Society of Petroleum Engineers.
- TAGAVIFAR, M., HERATH, S., WEERASOORIYA, U. P., SEPEHRNOORI, K. & POPE, G. 2018. Measurement of Microemulsion Viscosity and Its Implications for Chemical Enhanced Oil Recovery. *SPE Journal*, 23, 66-83.
- UNSAI, E., BROENS, M., BUIJSE, M., BOERSMA, D., MAKURAT, A. & ARMSTRONG, R. T. 2015. Visualization of Microemulsion Phase. *SPE Asia Pacific Enhanced Oil Recovery Conference*. Kuala Lumpur, Malaysia: Society of Petroleum Engineers.
- WALKER, D., BRITTON, C., KIM, D. H., DUFOUR, S., WEERASOORIYA, U. & POPE, G. A. 2012. The Impact of Microemulsion Viscosity on Oil Recovery. *SPE Improved Oil Recovery Symposium*. Tulsa, Oklahoma, USA: Society of Petroleum Engineers.
- WEGNER, J. & GANZER, L. 2017. Rock-on-a-Chip Devices for High p, T Conditions and Wettability Control for the Screening of EOR Chemicals. *SPE Europec featured at 79th EAGE Conference and Exhibition*. Paris, France: Society of Petroleum Engineers.
- WELLINGTON, S. L. 1983. Biopolymer Solution Viscosity Stabilization - Polymer Degradation and Antioxidant Use. *Society of Petroleum Engineers Journal*, 23, 901-912.
- WINSOR, P. A. 1954. *Solvent properties of amphiphilic compounds*, Butterworths Scientific Publications.
- YANG, D.-H., WANG, J.-Q., JING, L.-X., FENG, Q.-X. & MA, X.-P. 2010. Case Study of Alkali - Polymer Flooding with Treated Produced Water. *SPE EOR Conference at Oil & Gas West Asia*. Muscat, Oman: Society of Petroleum Engineers.
- YANG, S. H. & TREIBER, L. E. 1985. Chemical Stability of Polyacrylamide Under Simulated Field Conditions. *SPE Annual Technical Conference and Exhibition*. Las Vegas, Nevada: Society of Petroleum Engineers.
- ZHANG, X., HAN, M., FUSENI, A. & ALSOFI, A. M. 2017. A New Facile Approach to Estimate EOR Polymers Thermal Stability at Harsh Reservoir Conditions. *Abu Dhabi*

International Petroleum Exhibition & Conference. Abu Dhabi, UAE: Society of Petroleum Engineers.